UPPSALA
UNIVERSITET

Digital Comprehensive Summaries of Uppsala Dissertations from the Faculty of Science and Technology 1443

Numerical Modelling and Mechanical Studies on a Point Absorber Type Wave Energy Converter

YUE HONG

ACTA
UNIVERSITATIS
UPSALIENSIS
UPPSALA
2016

ISSN 1651-6214
ISBN 978-91-554-9731-6
urn:nbn:se:uu:diva-305650

Dissertation presented at Uppsala University to be publicly examined in 80101, Ångströmlaboratoriet, Lägerhyddsvägen 1, Uppsala, Wednesday, 7 December 2016 at 13:00 for the degree of Doctor of Philosophy. The examination will be conducted in English. Faculty examiner: Researcher Jørgen Hals Todalshaug (Norwegian University of Science and Technology).

Abstract
Hong, Y. 2016. Numerical Modelling and Mechanical Studies on a Point Absorber Type Wave Energy Converter. *Digital Comprehensive Summaries of Uppsala Dissertations from the Faculty of Science and Technology* 1443. 76 pp. Uppsala: Acta Universitatis Upsaliensis. ISBN 978-91-554-9731-6.

Oceans cover two thirds of the Earth's surface and the energy potential of ocean waves as a renewable energy source is huge. It would therefore be a tremendous achievement if the vast mechanical energy in waves was converted into a form of energy that could be used successfully by society. For years, scientists and engineers have endeavored to exploit this renewable energy by inventing various generators designed to transform wave energy into electrical energy. Generally, this sort of generator is called a Wave Energy Converter (WEC).

In this thesis, the research is based on the WEC developed in the Lysekil Project. The Lysekil Project is led by a research group at Uppsala University and has a test site located on the west coast of Sweden. The project started in 2002. So far, more than ten prototypes of the WEC have been deployed and relevant experiments have been carried out at the test site. The WEC developed at Uppsala University can be categorized as a point absorber. It consists of a direct-drive linear generator connected to a floating buoy. The linear generator is deployed on the seabed and driven by a floating buoy to extract wave energy. The absorbed energy is converted to electricity and transmitted to a measuring station on land.

The work presented in this thesis focuses on building a linear generator model which is able to predict the performance of the Lysekil WEC. Studies are also carried out on the damping behavior of the WEC under the impact of different sea climates. The purpose is to optimize the energy absorption with a specific optimal damping coefficient. The obtained results indicate an optimal damping for the Lysekil WEC which can be used for optimizing the damping control.

Additionally, the impact two central engineering design features (the translator weight and the stroke length) are investigated. The aim is to find a reasonable structural design for the generator which balances the cost and the energy production.

Keywords: linear generator, point absorber, numerical modelling, power production, optimal damping

Yue Hong, Department of Engineering Sciences, Electricity, Box 534, Uppsala University, SE-75121 Uppsala, Sweden.

ISSN 1651-6214
ISBN 978-91-554-9731-6
urn:nbn:se:uu:diva-305650 (http://urn.kb.se/resolve?urn=urn:nbn:se:uu:diva-305650)

Dedicated to my parents

List of Papers

This thesis is based on the following papers, which are referred to in the text by their Roman numerals.

I **Hong Y.**, Waters R., Boström C., Eriksson M., Engström J., Leijon M. (2014) Review on electrical control strategies for wave energy converting systems. *Renewable and Sustainable Energy Reviews*, 31:329–342

II **Hong Y.**, Hultman E., Castellucci V., Ekergård B., Sjökvist L., Soman D. E., Krishna R., Haikonen K., Baudoin A., Lindblad L., Lejerskog E., Käller D., Rahm M., Strömstedt E., Boström C., Waters R. and Leijon M. (2013) Status update of the wave energy research at Uppsala University. *Proceedings of the 10th European Wave and Tidal Energy Conference*, Aalborg, Danmark, 2-5 September, EWTEC2013

III Parwal A., Remouit F., **Hong Y.**, Francisco F., Castellucci V., Hai L., Ulvgård L., Li W., Lejerskog E., Baudoin A., Nasir M., Chatzigiannakou M., Haikonen K., Ekström R., Boström C., Göteman M., Waters R., Svensson O., Sundberg J., Rahm M., Strömstedt E., Engström J., Savin A. and Leijon M. (2015) Wave energy research at Uppsala University and the Lysekil Research Site, Sweden: A status update. *Proceedings of the 11th European Wave and Tidal Energy Conference*, Nantes, France, 6-11 September, EWTEC2015

IV **Hong Y.**, Eriksson M., Castellucci V., Boström C., Waters R. (2016) Linear generator-based wave energy converter model with experimental verification and three loading strategies. *IET Renewable Power Generation*, 10(3): 349-359

V **Hong Y.**, Eriksson M., Boström C., Waters R. (2016) A study on the damping coefficient of a direct-drive type wave energy converter, conditionally accepted to *Renewable Energy*, September, 2016

VI **Hong Y.**, Eriksson M., Boström C., Waters R. (2016) Impact of generator stroke length on energy production for a direct drive wave energy converter. *Energies,* 9: 730-742

Contents

Nomenclature and abbreviations

Chapter 2—Theory

Chapter 2.1

Symbol	SI unit	Description
f	Hz	Frequency
g	m/s^2	Acceleration of gravity
H	m	Wave height
H_s	m	Significant wave height
J	W/m	Energy flux
m_n	m^2/s^n	Spectral moment at the nth order
T_e	s	Energy period
$S(f)$	m^2s/rad	Wave power spectrum
S_{BS}	m^2s/rad	Bretschneider spectrum
ρ	kg/m^3	Density of the sea water
ω	rad/s	Angular frequency
ω_m	rad/s	Modal frequency for any given wave

Chapter 2.2

Symbol	SI unit	Description
f_{damp}	N	Damping force induced inside linear generator
f_h	N	Hydrostatic force
f_{exc}	N	Excitation force
f_{line}	N	Line force
f_{upp_es}	N	Spring force on upper end stop
f_{low_es}	N	Spring force on lower end stop
$h(t)$	$-$	Impulse response function for the radiation impedance
k_{line}	N/m	Spring constant of line
k_{s1}	N/m	Spring constant for the upper end stop
k_{s2}	N/m	Spring constant for the lower end stop
l_1	m	Stroke length to upper end stop
l_2	m	Stroke length to lower end stop
m_a	kg	Mass of the buoy
m_b	kg	Mass of the translator

m_∞	kg	Added mass in infinity frequency limit
P_{ratio}	%	Power capture ratio
$P_{absorbed}$	kW	Absorbed wave power from the absorber
$P_{available}$	kW	Wave power density
x_1	m	Buoy position
x_2	m	Translator position
γ	Ns/m	Damping coefficient
ϕ	m	Diameter of the buoy

Chapter 2.3

Symbol	SI unit	Description
A_{fac}	$-$	Reactive area between translator and stator
ε	V	Open circuit voltage
ε_a	V	Voltage drop on Phase A
ε_b	V	Voltage drop on Phase B
ε_c	V	Voltage drop on Phase C
i_a	A	Phase current flowing at A
i_b	A	Phase current flowing at B
i_c	A	Phase current flowing at C
k	$1/m$	Wave number
L	H	Inductance
N	$-$	Number of turns of the winding inside the stator
R_g	Ω	Resistance of generator windings
R_c	Ω	Resistance of the sea cable
R_{load}	Ω	Load resistance
R	Ω	Resistance
V_a	V	Phase Voltage output from the generator on phase A
V_b	V	Phase Voltage output from the generator on phase B
V_c	V	Phase Voltage output from the generator on phase C
V_g	V	Voltage drop over the generator resistance
V_{sea}	V	Voltage drop over the sea cable
V_{load}	V	Load voltage
ρ	kg/m^3	Density of the sea water
α	$-$	Factor for calculating the A_{fac}
β	$-$	Factor for calculating the A_{fac}
θ	rad	Phase angle
λ	m	Wave length
Φ	Wb	Magnetic flux
Φ_0	Wb	Magnitude of magnetic flux

Chapter 6—Impact by translator mass

Symbol	SI unit	Description
E_k	J	The kinetic energy of the translator
E_p	J	The gravitational potential energy on the translator
W_{damp}	J	The work done by the damping force
W_{line}	J	The work done by the force on the guiding line

Abbreviation	Description
AC	Alternating Current
DC	Direct Current
OWC	Oscillating Water Column
WEC	Wave Energy Converter

1. Introduction

The concept of the Wave Energy Converter (WEC) was first introduced the 70s [1]. It was originally a navigation buoy [2], which was designed to be self-powered by transforming the wave mechanics into electricity. Since then, the concept has been developed into a variety of advanced applications and even deployed in a large-scale project [3, 4, 5]. With increasing knowledge and experience, expectations are growing for wave energy plants to be able to open up the ocean's potential, and provide electricity by connecting to the grid. However, budgeting can be one of the trickiest parts of a project, especially with regards to the high cost of manufacturing, operating and maintaining a high power rating WECs [6]. Furthermore, to make the WECs competitive in the electricity market, it is necessary to be able to guarantee a stable power supply.

In this introduction, I briefly categorize different types of WECs, in line with one of my review articles PAPER I. This is followed by an outline of the Lysekil project [7, 8] which my research proposal is a part of. Lastly, the research aim is specified.

1.1 Wave energy technologies

Wave energy technologies vary wildly in the mechanical and electrical principal of operation [9]. In this study, the WEC devices are categorized based on their mechanics. More details and relevant electrical strategies can be found in PAPER I.

1.1.1 Oscillating water column

The oscillating water column (OWC) device consists of a partially submerged chamber with a water column that rises and falls in response to the pressure from the ocean waves [10, 11]. Both the upward and downward movement of the column drive air through a turbine and the turbine drives a generator for electricity production. One of the typical OWC devices is the Pico Plant on the Azores in Portugal [12], see Figure 1.1(a).

1.1.2 Overtopping devices

Overtopping devices are partially submerged wave energy converters with reservoirs for capturing wave crests and water turbines to produce electricity. The kinetic energy of the waves is converted into potential energy when incoming waves are led up a ramp and water is collected in a reservoir [13]. The water returns to the ocean from the reservoir through water turbines, thus utilizing the potential difference between the ocean and the reservoir to generate electricity. The Wave Dragon [14, 15] deployed and tested offshore in Denmark, as shown in Figure 1.1(b) is a famous example of an overtopping device.

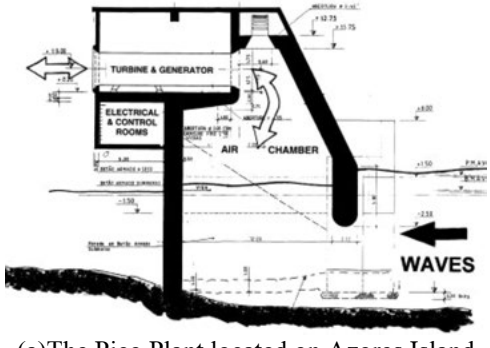

(a)The Pico Plant located on Azores Island in Portugal [12].

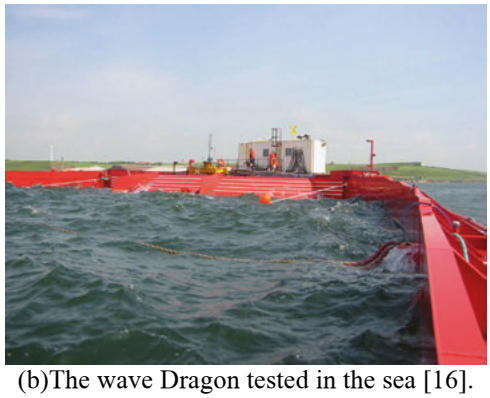

(b)The wave Dragon tested in the sea [16].

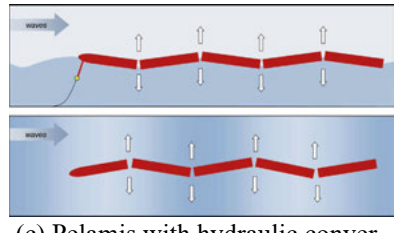

(c) Pelamis with hydraulic conversion system [22].

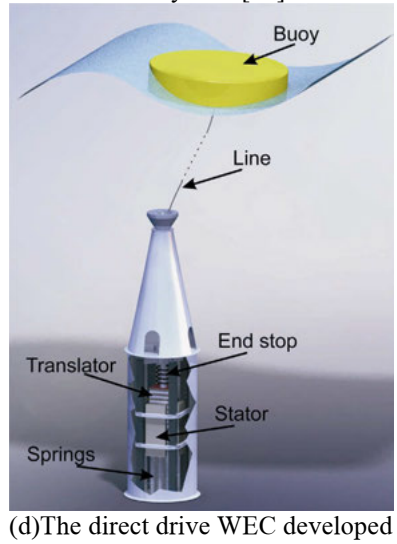

(d)The direct drive WEC developed in the Lysekil Project (courtesy of Rafael Waters).

Figure 1.1 Illustration on different types of WECs (reused from PAPER I).

1.1.3 Attenuators

Attenuators are devices where the water physically pushes and induces motion in the WEC's structure and energy is converted by dampening this motion [17, 18]. The devices are often constructions that float on and interact with the ocean waves without being physically fixed in place.

Attenuators can be categorized into two types: hinged attenuators and point absorbers [19].

a. Hinged attenuators

Hinged attenuators consist of several parts linked horizontally by universal joints, allowing flexing movement in multiple directions. The Pelamis for instance, is a device that floats semi-submerged on the surface of the water and faces the direction of waves [20, 21], see Figure 1.1(c). As waves pass down the length of the machine and the sections bend in the water, the movement is converted into electricity via hydraulic systems. The power is then transmitted to the grid on the shore.

b. Point absorbers

Point absorbers are usually smaller than other WECs. Point absorbers are equipped with a floating part which enables a heave motion driven by the waves, and a generator which is connected to the floating structure and which converts the mechanics into electricity [23]. As illustrated in Figure 1.1(d), the Lysekil WEC developed in Sweden is a typical example [24].

1.2 Lysekil Project

1.2.1 Test site

The Lysekil Project is one of the world's ongoing wave energy research projects, aiming to develop a WEC farm will full scale devices for Swedish conditions and study wave energy conversion [25]. This project is led by a research group from the division for electricity at Uppsala University [26]. The test site is located offshore, in Västra Götaland county, on the west coast of Sweden (58.18N, 11.37E). Several points make this location suitable as a test site [27]:

a. A flat and wide sea bottom with an average depth of around 25 meters. This condition makes it possible to accommodate over 10 WECs.
b. The nearby island Härmanö provides convenient transportation possibilities and enables connection to the gird on the surrounding island.
c. The nearby city of Lysekil has a well-equipped harbor and serves as a starting point for the deployments of WECs and other large scale equipment.

1.2.2 History

The project started in 2002 [28] and has developed into a multi-physics platform for different research programs [29]. The project's first WEC, named the L1, was installed and connected to an onshore load in March 2006 [30, 31].

During the last ten years, over ten different prototypes of the WECs and two marine substations [32, 33] have been deployed at the test site.

The first generator (L1) was installed with the purpose of verifying the concept of the WEC. After the installation of the L2 and the L3 in 2009, the three generators were connected into a farm through a marine substation [34]. The converted electricity was transferred to an onshore measuring station. The L2 and the L3, had an updated measurement system, as well as an improved mechanical design. At the end of 2009, a new linear generator, the L9, was deployed at the site [35]. The L9 had an updated design, aimed at obtaining a higher power production. In November 2010, four generators (L4, L5, L7 and L8) with various designs were installed. The L7 was connected to a resonant electrical circuit for rectification, while the L8 was connected to a diode rectifier. In 2015, three different generators (L10, L11 and L12) were launched as well as an advanced marine substation equipped with auxiliary control modules [36, 37, 38].

A variety of buoys have been developed and tested for the connection to the generators. So far, three types of buoys have been developed and investigated: cylindrical buoys, torus buoys and discus buoys [25, 39, 40]. Both force sensors and accelerometers have been installed in the buoys.

A measuring station was built to provide a platform for the load tests [41]. From 2006 to 2008, the WECs were connected with resistive loads and a passive rectified circuit [42, 43]. In 2010, a resonant circuit was designed to upgrade the power production [44, 45] and the electrical system has been continually upgraded since then, currently e.g. hosting full AC/DC/AC conversion and grid connection.

The project also has a number of ongoing interdisciplinary studies, such as studies on the cooling systems for the substations [46, 47, 48], remotely operated vehicles [49] and buoys that can alter the length of the buoy line in response to sea level variations [50, 51]. All aim to improve the overall viability of the WEC concept. Furthermore, there are studies on different areas of environmental impact [52, 53, 54]. An observation tower was built during 2007 and 2008 to monitor the test site as well as collecting wave data with the wave measuring buoys [55]. At the same time, biology buoys were deployed to study the biofouling and the impact from the WECs on the marine environment [56].

1.2.3 Previous work with published thesis

At present, 20 PhD theses have been published by the wave energy research group at Uppsala University. A brief summary of the contributions is provided here.

Dr. Thorburn proposed an electrical approach on the concept of Wave Energy Conversion focused on the modelling of rectification and transmission of the generated electricity [57].

Extensive studies on the linear permanent magnet generator designed for the studied WEC concept was carried out by Dr. Danielsson [58].

Dr. Eriksson proposed and verified a hydrodynamic model on the interaction between the point absorbing type WEC and the ocean waves [59].

Dr. Waters main contribution was a mechanical design and the construction of the first full scale linear generator (the L1). Experiments on the prototype were carried out over several years. [60].

The environmental impact caused by the WEC on the marine ecosystem was carried out by Dr. Langhamer [61].

The first marine substation for electrical conversion and connection of up to three WECs in a small wave farm was designed by Dr. Rahm [62].

Dr. Lindroth performed research on the L1's in the presence of changing water levels, wave heights and how the WEC behavior corresponded to the spectral shapes of different sea states [63].

A two-body system WEC was proposed by Dr. Engström, presenting a option for enhancing the wave energy capture ratio [64].

Different load strategies of the WECs were studied by Dr. Boström both in modelling and experiments at the Lysekil test site [65].

Force measurements on the buoy and measurement systems in the substation and measuring station were installed by Dr. Svensson [66].

Dr. Strömstedt studied the linear lead through for the WEC and performed extensive measurements on the WECs [67].

Dr. Andrej studied the reliability of the mechanical parts of the linear generator as well as the lateral forces acting on the outer structure of the WEC [68].

A new type of linear generator equipped with ferrite permanent magnets was studied by Dr. Ekergård [69].

Dr. Ekström developed a marine substation, for up to 7 WECs, equipped with advanced measuring and control systems [70].

Dr. Gravråkmo investigated the point absorbing buoys with respect to their different geometry, size and hydrodynamic performance [40].

Dr. Haikonen conducted research on the radiated noise from the WEC and possible impact to the marine environment [71].

The electrical conversion of a three-level inverter from WEC to the grid was studied by Dr. Krishna [72].

Dr. Hai proposed an approach on equivalent circuit modelling to simulate the performance for the WEC developed in the project [73].

Dr. Lejerskog performed a study on the cogging forces generated inside the generator. He also studied new generator designs [74].

A sea level compensation system was developed by Dr. Castellucci aiming to optimize the energy extraction from the ocean waves in areas with high tides [75].

1.3 Aims of thesis

My research aim has been focused on developing and using WEC models to study the energy conversion of the chosen WEC concept. The performance of the WECs is investigated by varying the mechanical design, aiming to optimize the energy absorption.

2. Theory

This chapter begins with a basic theory on the wave energy spectrum. The hydrodynamic theory is proposed in the second paragraph to illustrate the interaction between the waves and the WEC device. This theory is important to predict the WEC behavior and energy extraction by solving the mechanical relationships. The theory is applied when building the numeric model, as well as to perform the studies in Papers V and VI on the WEC device.

Later in this chapter, the electrical theory on the linear generator is proposed and a WEC model is developed based on it. The theory is explained in paper IV. Furthermore, three load strategies for practical tests in the Lysekil project are presented and simulated with the proposed WEC models.

2.1 Ocean waves and energy spectrum

Ocean waves, regarding as the irregular waves, can be defined by the wave height H, wave length λ and wave period T, see Figure 2.1. On the premise that the linear theory is applicable [76] when the water depth $h > 2\lambda$ [77], the irregular waves is concerned as a superposition of series of different frequencies. An analysis approach of the wave spectrum $\mathrm{S}(f)$ is commonly utilized to describe the real sea state, where f is the frequency [78]. The n^{th} moment if the spectral density in continuous form is interpreted in Equation (2.1),

$$m_n = \int_0^\infty f^n S(f)\, df \tag{2.1}$$

The significant wave height and average energy period are expressed respectively as below,

$$H_s = 4\sqrt{m_0} \tag{2.2}$$

$$T_e = m_{-1}/m_0 \tag{2.3}$$

According to (2.1) under the deep water condition [79], the energy flux for the real ocean waves could be then obtained:

$$J = \frac{\rho g^2}{64\pi} T_e H_s^2 \tag{2.4}$$

where ρ is the density of the sea water and g is the acceleration of gravity.

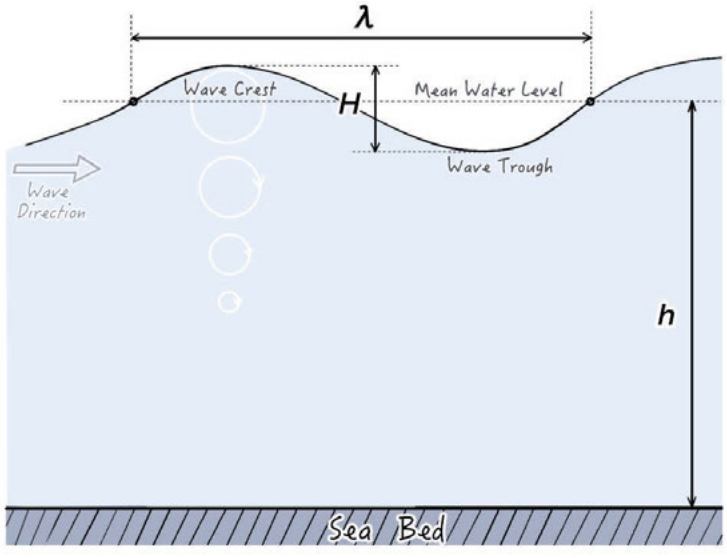

Figure 2.1. a simple definition of the ocean wave's characteristics with wave length λ, wave height H and water depth h.

In addition, the Bretschneider spectrum [80] is also used as one of the empirical approaches to describe the ocean waves, defined as below,

$$S_{BS}(\omega) = \frac{5}{16}\frac{\omega_m^4}{\omega^5}H_s^2 e^{-5\omega_m^4/4\omega^4} \tag{2.5}$$

In Equation (2.5) where ω is the angular frequency, ω_m is the modal frequency for any given wave. Figure 2.2 gives an example of the Bretschneider spectrum used for describing five different sea states.

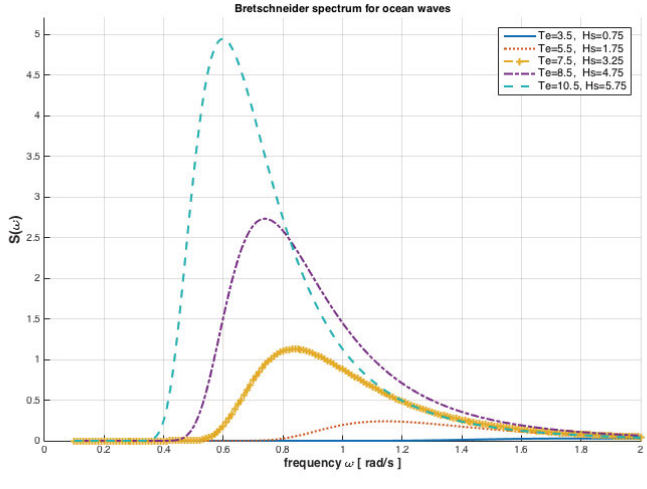

Figure 2.2. An example of Bretschneider spectrum describing the ocean waves by known wave period and significant wave height.

2.2 Hydrodynamics model

The mechanic interaction between a Wave Energy Converter and the waves is described in Equation (2.6). In this study, the floating buoy is restricted to the heave motion only. In Equation (2.6), x_1 is the vertical position of the buoy and x_2 is the translator position under excitation from the waves. The upper differential equation describes the interaction between the buoy and the waves, where m_a is the mass of the buoy, m_∞ is the added mass in infinity frequency limit, f_{exc} is the time dependent excitation force, $h(t)$ is the impulse response function for the radiation impedance, f_h is the hydrostatic force and f_{line} is the line force.

$$\begin{cases}(m_a + m_\infty)\ddot{x}_1 = f_{exc}(t) - h(t)\dot{x}_1(t) - f_h - f_{line}(x_1, x_2) - m_a g \\ m_b\ddot{x}_2 = f_{line}(x_1, x_2) + f_{damp}(x_2, \dot{x}_2) - m_b g + f_{upp\_es} + f_{low\_es}\end{cases} \tag{2.6}$$

The lower differential equation describes the motion of the translator driven by the buoy, where m_b is the translator mass and f_{damp} is the generator damping force. The end stops are springs with a high spring constant, denoted as f_{upp_es} and f_{low_es} respectively in the equation. The line between the buoy and the translator is modelled as a stiff spring, which becomes active when the distance between buoy and translator becomes larger than the length of the line. The line force is modelled by Equation (2.7), where the spring constant is denoted as k_{line}.

$$f_{line}(x_1, x_2) = \begin{cases} k_{line}(x_1 - x_2) & if\ \ x_1 > x_2 \\ 0 & else \end{cases} \tag{2.7}$$

The upper and lower end stop forces are described in Equation (2.8) and (2.9). In the equations where k_{s1} and k_{s2} are the spring constant for the end stops, l_1 and l_2 are the stroke length to the upper and lower end stop respectively.

$$f_{upp\_es}(x_2) = \begin{cases} -k_{s1}(x_2 - l_1) & if\ \ x_2 > l_1 \\ 0 & else \end{cases} \tag{2.8}$$

$$f_{low\_es}(x_2) = \begin{cases} -k_{s2}(x_2 - l_2) & if\ \ x_2 < -l_2 \\ 0 & else \end{cases} \tag{2.9}$$

The generator damping force is proportional to the translator speed with the damping coefficient γ, is given by.

$$f_{damp}(\dot{x}_2) = -\gamma\dot{x}_2 \tag{2.10}$$

The ratio between average absorbed power and the power transport towards the buoy is defined as the power capture ratio. The expression for the power capture ratio is given by,

$$P_{ratio} = \frac{P_{absorbed}}{P_{available}} \times 100\% \tag{2.11}$$

Where $P_{absorbed}$ is the average absorbed power by the buoy and $P_{available}$ is given by,

$$P_{available} = \phi \frac{\rho g^2}{64\pi} T_e {H_s}^2 \tag{2.12}$$

where the buoy diameter is denoted by ϕ, while T_e and H_s is the mean energy period and the significant wave height respectively.

2.3 Electrical theory of linear generator model

In the linear generator, the magnetic flux is generated by the permanent magnets on the translator. The flux is confined inside the magnetic path along the laminated steel sheets, enclosing the isolated conductors mounted on the stator [81]. Assuming that the magnetic flux has a sinusoidal form, the flux can be described as

$$\Phi = \Phi_0 sin\,(kx_2 + \theta) \tag{2.13}$$

In the equation above, k is the wave number, $k = \frac{2\pi}{\lambda}$, λ is the wave length. Φ_0 is the magnitude of the magnetic flux, x is the position of the translator, and θ is the phase angle. If the position is time-dependent, the flux can be derived with respect to time,

$$\frac{d\Phi}{dt} = k\Phi_0 cos\,(kx_2 + \theta) \cdot \frac{dx_2}{dt} \tag{2.14}$$

According to Faraday's Law [82], when the magnetic flux is induced and flows through the path of a magnetic circuit, a voltage is induced according to the rate of change of the magnetic flux. The induced open circuit voltage is expressed as,

$$\varepsilon = -N\frac{d\Phi}{dt} \tag{2.15}$$

where N is the number of turns of the cable winding inside the stator.

Inserting Equation (13) into the right side of Equation (14), it gives,

$$\varepsilon = -Nk\Phi_0 cos(kx_2 + \theta) \cdot \frac{dx_2}{dt} \tag{2.16}$$

For a three-phase generator, like the L9, the induced three-phase voltage is described by a system of Equations (2.17).

$$\begin{cases} \varepsilon_a = -Nk\Phi_0 cos(kx_2) \cdot \frac{dx_2}{dt} \\ \varepsilon_b = -Nk\Phi_0 cos(kx_2 + \frac{2\pi}{3}) \cdot \frac{dx_2}{dt} \\ \varepsilon_c = -Nk\Phi_0 cos(kx_2 - \frac{2\pi}{3}) \cdot \frac{dx_2}{dt} \end{cases} \quad (2.17)$$

In the generator, the output voltage is also influenced by the active area between the stator and translator. The area represents the portion of the magnetic circuit that contributes to the induced voltage. The A factor is used to describe how much surface of the stator is active between the translator and stator. The A factor is depending on the position of the translator's central point instead.

Figure 2.3. An illustration of the A factor's relation to α and β.

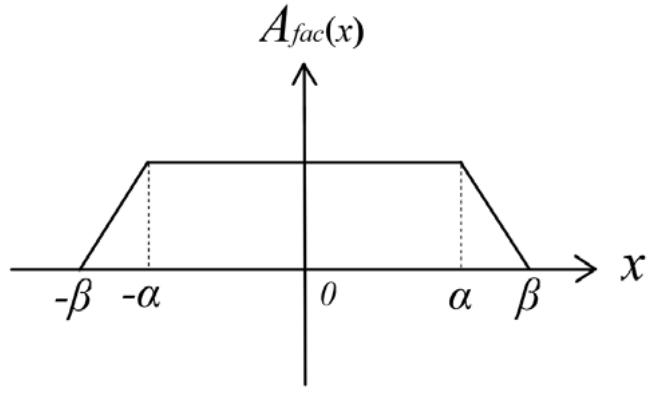

The system of Equations (2.18), shows how the A factor varies with respect to the position of the translator's central point x, as illustrated in Figure 2.3.

$$A(x_2)_{fac} = \begin{cases} 1 & |x_2| < \alpha \\ \frac{1}{\alpha-\beta}(|x_2| - \alpha) + 1 & \alpha < |x_2| < \beta \\ 0 & |x_2| > \beta \end{cases} \quad (2.18)$$

According to Kirchhoff's Law for a star-connected generator, the voltages have to fulfil the system of Equations (18)

$$\begin{cases} \varepsilon_a A(x_2)_{fac} = Ri_a + L\frac{di_a}{dt} + V_a \\ \varepsilon_b A(x_2)_{fac} = Ri_b + L\frac{di_b}{dt} + V_b \\ \varepsilon_c A(x_2)_{fac} = Ri_c + L\frac{di_c}{dt} + V_c \end{cases} \quad (2.19)$$

Taking the linear generator L9 as an example, factor α and β are $\alpha = 0$, $\beta = 2$, then the A factor can be calculated as:

$$A(x_2)_{fac} = \begin{cases} 0 & |x_2| > 2 \\ 1 - \frac{1}{2}|x_2| & 0 < |x_2| < 2 \end{cases} \tag{2.20}$$

The damping force is calculated out by using Equation (2.10) as below:

$$f_{damp} = \gamma(\dot{x}_2)A_{fac}(x_2)\dot{x}_2(t) = 3\left[\frac{1}{R_g}\left(\frac{V_g}{\dot{x}_2}\right) + \frac{1}{R_c}\left(\frac{V_{sea}}{\dot{x}_2}\right) + \frac{3}{R_{load}}\left(\frac{V_{load}}{\dot{x}_2}\right)^2\right] \tag{2.21}$$

where γ, V_g, V_{sea}, and V_{load} are, respectively, the damping coefficient, the voltage drops over the resistances of the generator, the sea cable, and the load.

2.4 Load strategies for generator

At the Lysekil research site, off the Swedish west coast, three cases of load strategies have been applied in experiments. They are the linear load, passive rectification and the resonant circuit. More details are presented in [65].

2.4.1 Linear load

The linear load is a three-phase star-connected resistive load, as shown in Figure 2.4. This basic load was first applied to the WECs, in order to observe the output profile and the performance of the WEC.

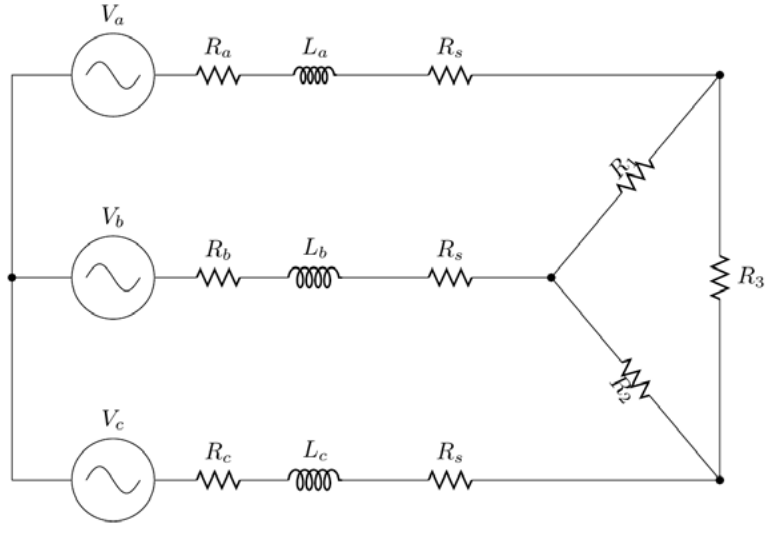

Figure 2.4. A basic circuit of a wye-connected linear generator and a delta-connected load.

2.4.2 Passive rectification and filter

A three-phase diode-bridge was used as a full-wave rectifier, converting the AC voltage generated from the L9 generator into a DC voltage [83]. The corresponding circuit diagram is shown in Figure 2.5. A π-section filter is applied at the DC side. This circuit is built and connected to the linear generator model in the simulation to observe the response.

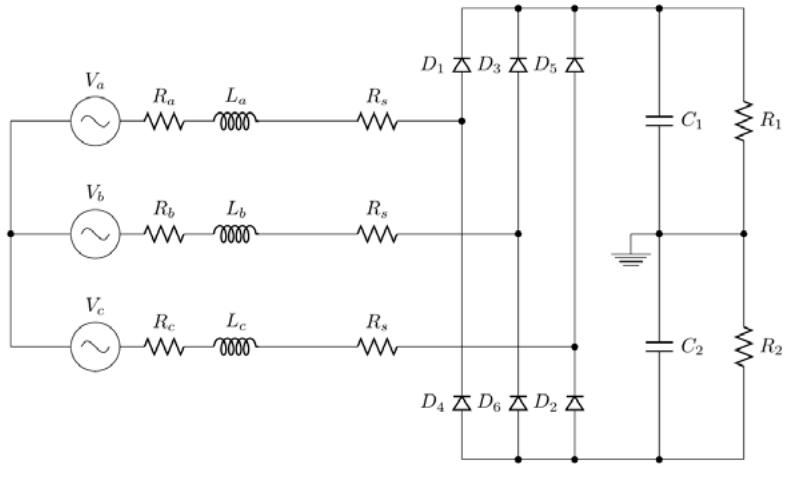

Figure 2.5. Circuit diagram of the passive rectified circuit and filters connected to the linear generator.

2.4.3 Resonant rectification

The resonant circuit was previously developed by C. Boström [84] at Uppsala University and has been tested at the Lysekil research site. Figure 2.6 shows one phase of the circuit diagram. The purpose of the circuit is to increase the damping factor and thus to extract more wave energy and deliver more power to the load compared to the passive rectification case. More details about the design and the theory of the circuit are provided in the reference [85].

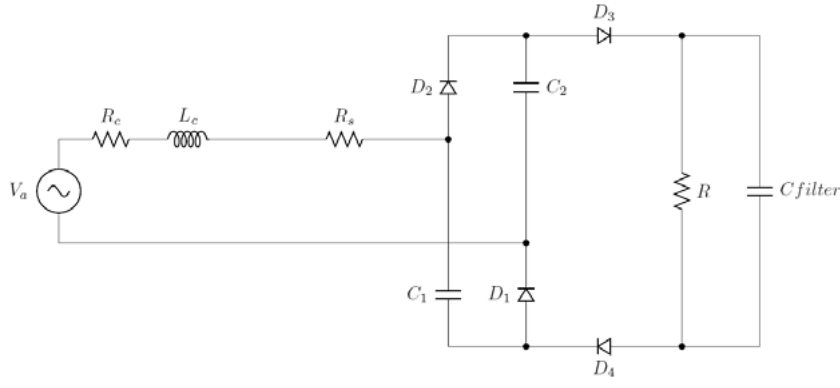

Figure 2.6. Circuit diagram of one phase of the resonant circuit.

3. Material and Method

3.1 Wave climates at test site

In this study, irregular waves are used for the WEC modelling. The data are from one of the Lysekil test sites at the Swedish west coast. The wave facts used in this study were purchased from Fugro OCEANOR of Norway [86].

Figure 3.1(a) is a map representing the location of the test sites studied by the Lysekil Project. Site 9 is the location of the actual experimental test site. The documented wave climates at Test Site 6 was used in the models studied in this thesis. A scatter diagram including the energy content in the waves is illustrated in Figure 3.1(b). The scatter diagram is from a previous study by R. Waters et al [87]. In the figure, the values displayed on the scattered squares are the accumulated hours for each sea during one year and the colours represent the annual available energy for the combinations of wave height and period.

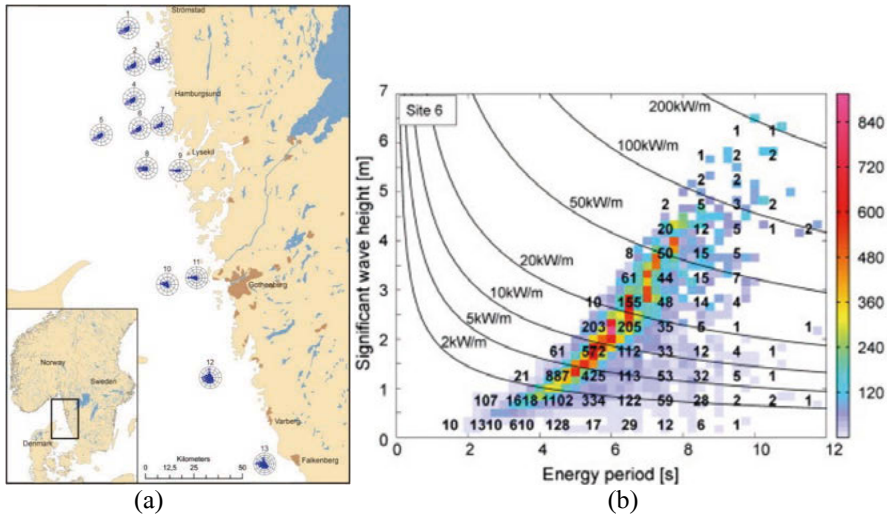

(a) (b)

Figure 3.1. Map and sea states at Test Site 6 studied by the Lysekil Project: (a) Map depicting the location of the studied sites. The wave roses are placed with their centre on the studied sites and show the distribution in time of the direction of the incoming waves; (b) Combined scatter and energy diagrams for Test Site 6. Colours show the annual energy transport per meter of wave front (kWh/year). Numbers give the average occurrence in hours per year. These two figures are cited from a published research article [87].

3.2 Device parameters

For the simulation, the model parameters are taken from the prototype L9 developed in the Lysekil project. Parameters relating to the Wave Energy Converter are listed in Table 3.1.

Table 3.1. the WEC (L9) specifications

Specifications of L9	
Nominal power at 0.7m/s	20 kW
Generator resistance	1±1.5%Ω
Generator inductance	20mH
Vertical stator length	2m
Vertical translator length	2m
Translator weight	2700kg
Buoy diameter	4m
Buoy weight	6300kg

3.3 Simulation tools

This study uses the software MATLAB as the platform for the all the modelling, as well as its Toolbox SIMULINK and GUI. Taking Figure 3.2 as an example, it presents an interface built in GUI for the numeric WEC model. The interface provides a convenient monitor and control by adjusting the parameters on the menu. Figure 3.2(a) displays the irregular wave (Te= 4s, Hs=7]) introduced by the hydrodynamic model, in addition to a subplot of the wave spectrum.

Figure 3.2(b) gives a displacement of the translator under the wave climate shown in Figure 3.2. Several WEC parameters can be adjusted in the menu, including the damping coefficient, the translator mass, the stroke length and the buoy size.

The linear generator is built by using the toolbox SIMULINK. Figure 3.3 gives a layout of the linear generator model with the load connection. On the left side, the boxes are built up according to the different functions to be achieved of the study.

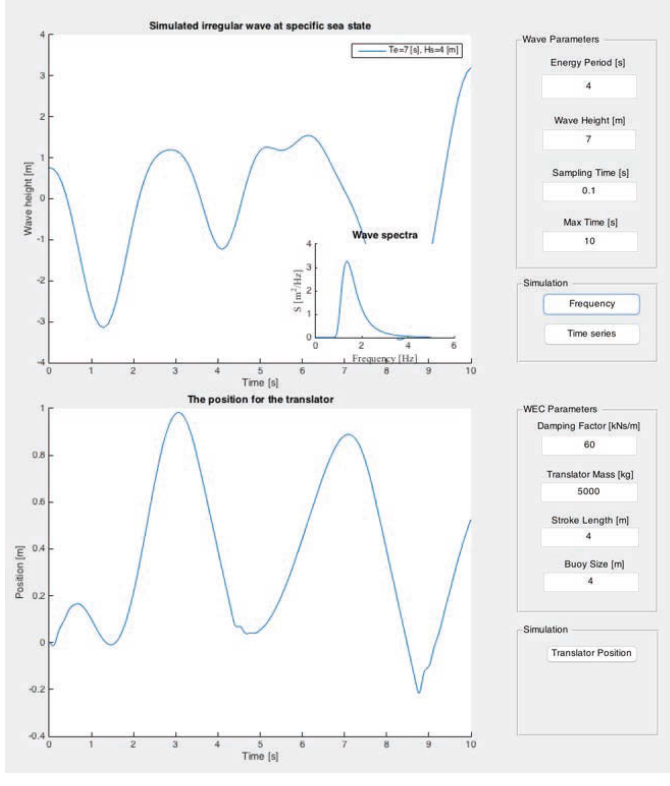

Figure 3.2. The interface of the WEC models with parameters option.

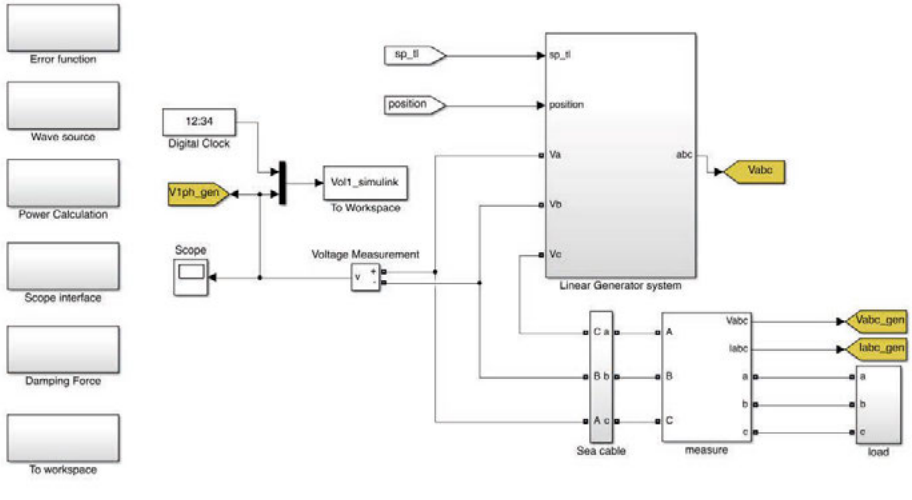

Figure 3.3. A layout of the linear generator model connected to a load system in Matlab Simulink.

4. Linear Generator Model

The numeric modelling of a WEC has an important role in designing a competitive WEC and predicting its future performance under various circumstances. A good model can help to lower the cost of the device. Mechanical parameters for the device can be adjusted conveniently in the model and it will be much easier to observe the impact of different engineering decisions. This is a considerable economic advantage, especially compared to the price of developing a new device or designing and carrying out a new offshore experiment.

The linear generator model, as a means of transforming wave energy into electrical energy production, provides a vital platform for the whole performance of the WEC model. In this section, the WEC model is proposed and the linear generator model is validated with the experimental results from the research project. Furthermore, the generator model will integrate the hydrodynamic model and three different load systems to study the overall performance of the WEC model.

4.1 Validation of linear generator model

The WEC model consists of two parts, a buoy floating on the surface and a linear generator on the seabed. The floating buoy is connected to the generator with a line. Electrical power is generated by the relative motion between a fixed stator and a movable translator, as illustrated in Figure 4.1. There are two end stops installed inside the generator to protect the generator from damage during rough wave conditions.

To provide proper support for designing a WEC device, it is necessary to build the model as realistic as possible. In that case, the numeric WEC model should be tested and proved to match the WEC prototype. In this study, the generator model is validated by comparing its simulated results with the experimental results.

Figure 4.2 gives the results of the validation of the linear generator model. Figure 4.2(a) presents the experimental result from one Lysekil WEC (L9), showing the displacement of the translator's central point under realistic wave climates in a time frame of 60s. By connecting to a star-connected resistive load, the simulated voltage from the model is obtained and further compared to the experimental voltage, displaced in Figure 4.2(b). Figure 4.2(c) shows the comparison during a time frame of 30s. Note that there are some obvious errors between the compared data, for example, the error occurred at 46.6s in

Figure 4.2(c). Error analysis is performed in the section of Discussion, and more details on the validation can be found in PAPER IV.

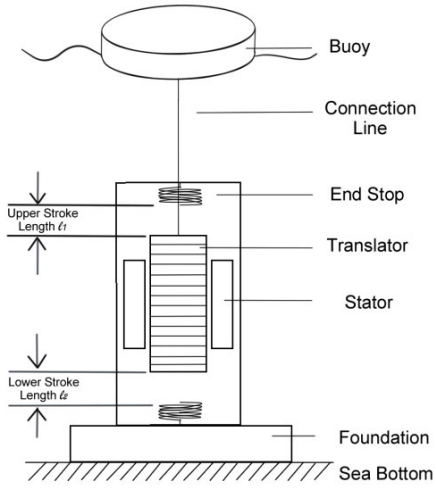

Figure 4.1. A simplified diagram of a direct-drive type WEC device.

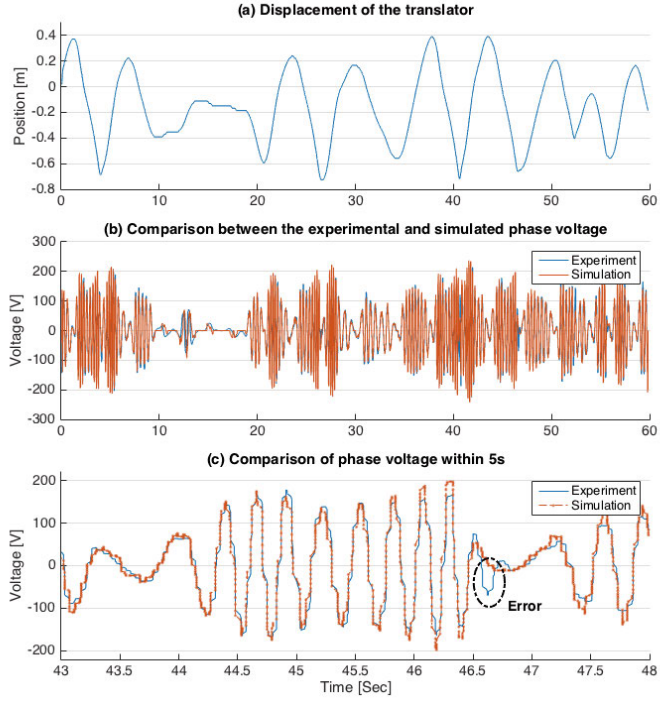

Figure 4.2. Output phase voltage from the linear generator model corresponding to the translator's displacement: (a) Displacement of the translator; (b) Comparison of the phase voltage between the experimental result and the simulated result; (c) a drawn-out comparison of Figure (b) within a time span of 5s. Similar results are presented in PAPER IV.

4.2 Hydrodynamic wave

In this study, a hydrodynamic model is used with the generator model. The hydrodynamic model was designed by Mikael Eriksson and gives both regular and irregular waves as a source to drive the generator model, as presented by Figure 4.3.

In this study, the harmonic waves are used as an elementary tool for the WEC's model, in order to provide a regular source for a regular voltage output. In this case, the voltage obtained is used as feedback to verify the parameters in the model. Irregular waves are used as a second step after the harmonic waves. Irregular waves simulate a realistic wave environment and drive the generator model to produce the uneven electrical power that is generated under such circumstances. Figure 4.3 shows a case with a significant height of 0.75m and an energy period of 3.5s.

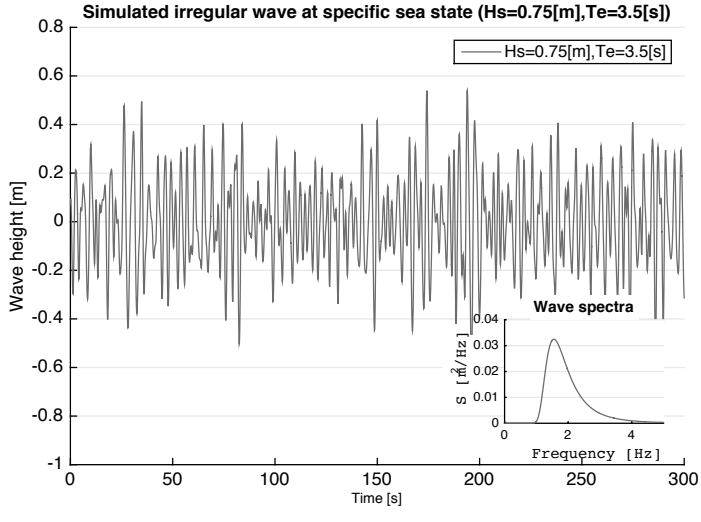

Figure 4.3. Wave source from the hydrodynamic model (a) the harmonic wave; (b) the irregular wave with a subplot of the wave spectrum.

4.3 Connection to load cases

For the following case studies, both harmonic waves and irregular waves are applied as the driving force of the WEC model. There is a parallel comparison for the three cases with harmonic waves. Also, for the studies with irregular waves, the three cases are all investigated with one identical irregular wave (Te=6s, Hs=2m).

4.3.1 Resistive load

A star-connected three-phase resistive load is used as the linear load. The purpose is to observe the voltage and the current profile of the generator, both under the conditions of harmonic waves and irregular waves. The results are presented in Figure 4.4 for the harmonic waves and Figure 4.5 for the irregular waves (Te=6s, Hs=2m).

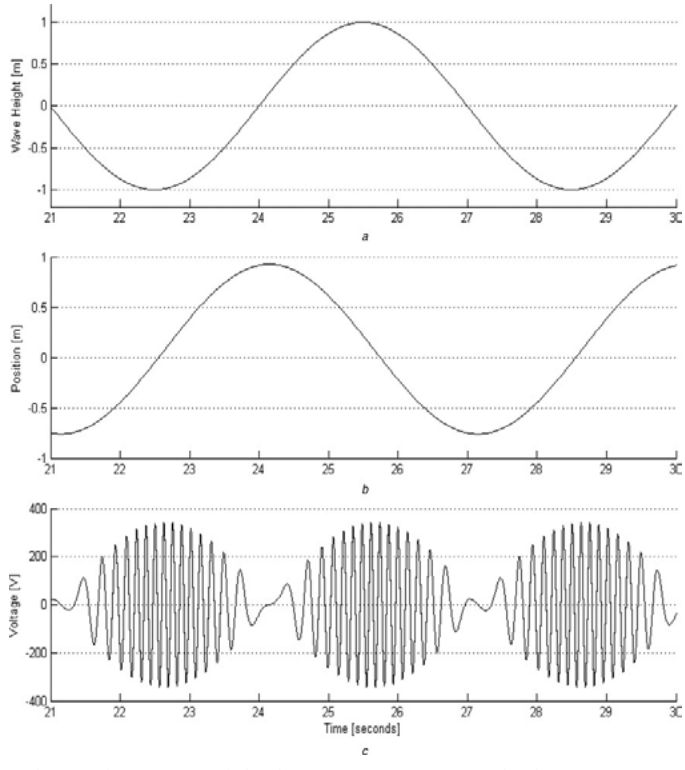

Figure 4.4. The performance of the linear generator: (a) the harmonic waves, (b) the displacement of the translator and (c) the phase voltage.

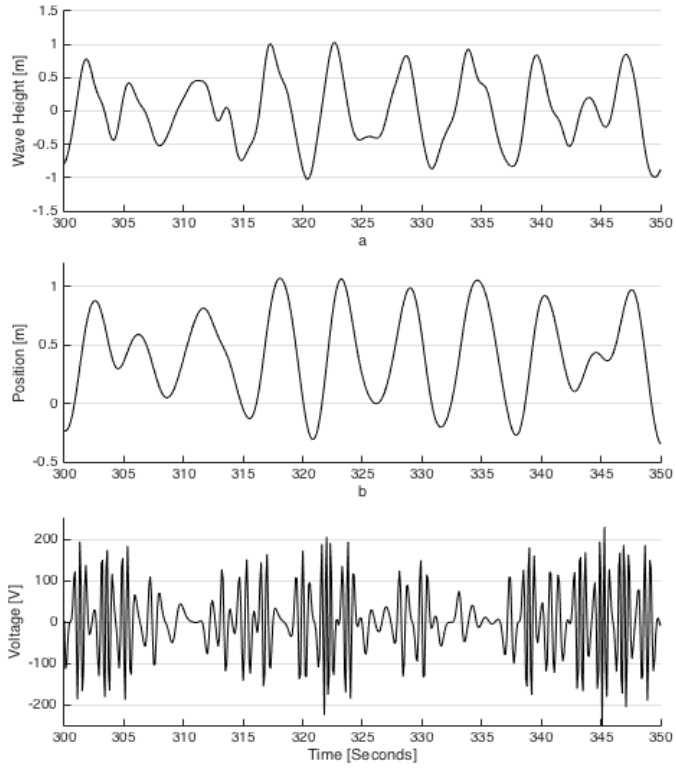

Figure 4.5. The performance of the linear generator: (a) the irregular waves, (b) the displacement of the translator and (c) the phase voltage.

4.3.2 Passive rectifier circuit

Figure 4.6 and Figure 4.7 present the results from the model connected to the passive rectifier circuit. In Figure 4.6, the WEC is working under harmonic waves, while the results in Figure 4.7 are from irregular waves. Besides the load, the DC voltage and the current from the rectification also depend on the initial voltage of the capacitive filters.

4.3.3 Resonant circuit

Some results from the study on the resonant circuit are presented in Figure 4.8 and Figure 4.9, for the harmonic waves and the irregular waves respectively. By comparing Figure 4.6, and Figure 4.8, it can be observed that the phase current of the resonant circuit has a higher amplitude than that of the rectifier circuit. However, the load voltage is much more stable for the passive rectification case. This is due to the large capacitors used as a filter. Furthermore, the same result for the case with irregular waves.

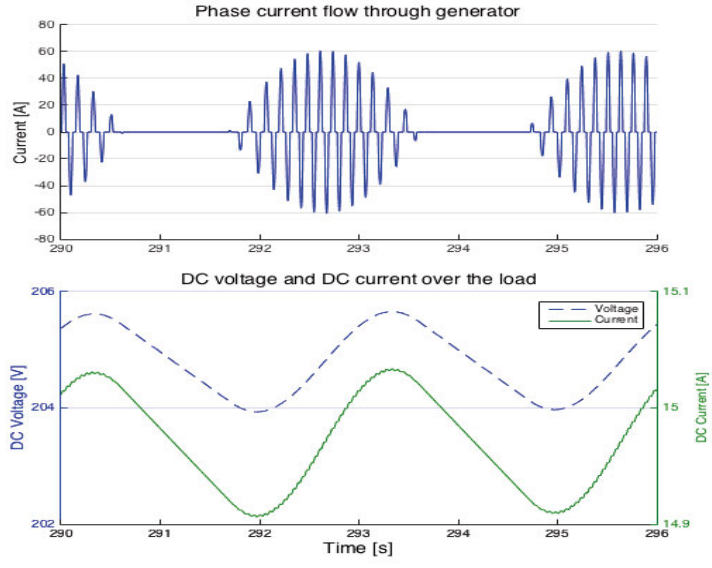

Figure 4.6. Simulated outputs from the generator, connected to passive rectifiers and capacitive filters, under harmonic waves: (a) Phase current flowing through the generator; (b) the DC voltage over the loads and the load currents.

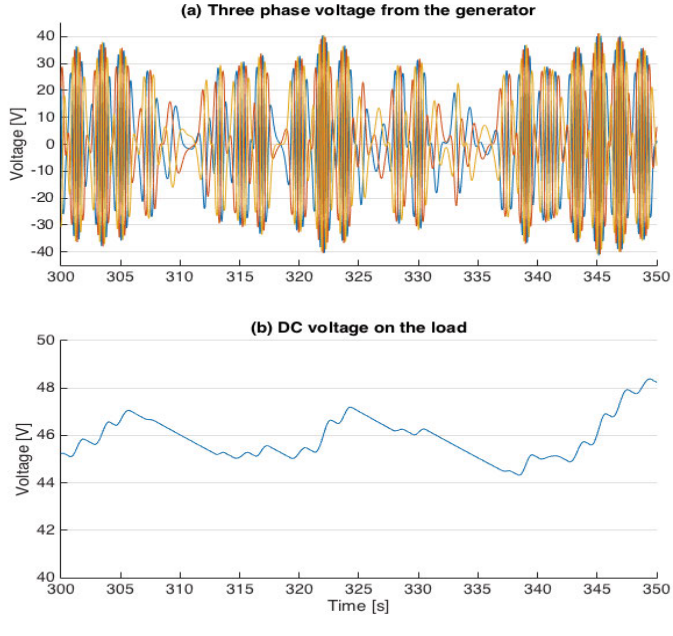

Figure 4.7. Simulated outputs from the generator, connected to passive rectifiers and capacitive filters, under irregular waves: (a) three phase voltage from the generator; (b) the DC voltage over the load after rectification.

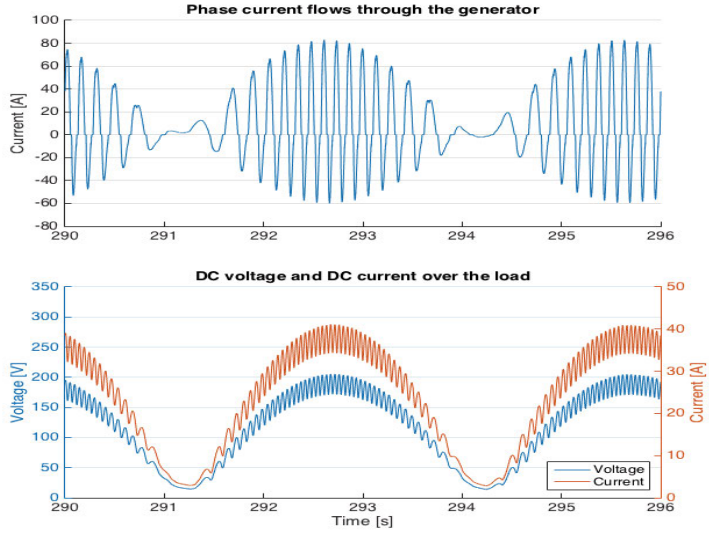

Figure 4.8. Outputs from the generator connected to the resonant circuit with harmonic waves: (a) Phase current through the generator; (b) load voltage and load current.

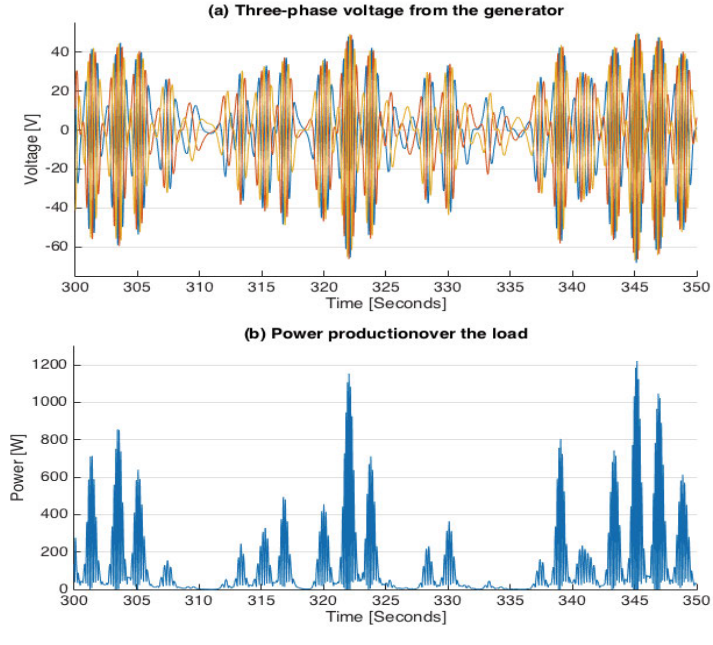

Figure 4.9. Outputs from the generator connected to the resonant circuit with irregular waves: (a) three-phase voltage from the generator; (b) the power production on the load.

5. Optimal Damping Coefficient

5.1 Different sea states and linear damping

To study the impact of the damping coefficient on the generator's performance, modelling is done by varying the value of the damping coefficient from 5 kNs/m to 190 kNs/m. Thus, a power profile can be obtained for a specific wave climate. In this study, 12 different sea states are used as the input source, to be able to observe the pattern of the profiles better. Figure 5.1 plots the power profiles for all 12 sea states.

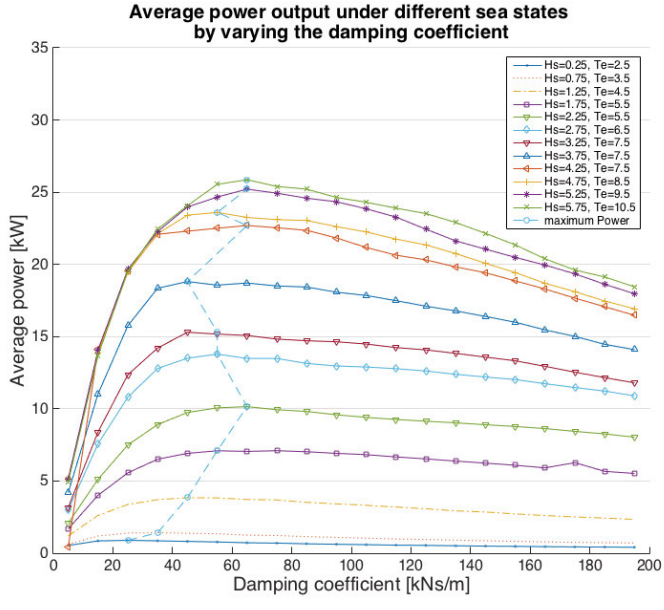

Figure 5.1. Generated power profile in response to the varying damping coefficients for 12 different sea states.

In Figure 5.1, a similar pattern can be found for the 12 different power profiles. For each profile, there is a maximum power point, which relates to an optimal damping coefficient. The power profiles get closer to each other as the waves becomes harsher. For instance, the difference in the power profile between [3.5s, 1.25m] and [5.5s, 1.75m] is much bigger than that between [9.5s, 5.25m] and [10.5s, 5.75m]. Moreover, the power production for all the profiles drops

slowly after the maximum power point even for a large increase in the value of the damping coefficient.

To provide a better view of the optimal damping, the results in Figure 5.1 are classified into three groups based on the levels of the sea state, as shown in Figure 5.2. A narrow damping interval, 45 kNs/m to 75 kNs/m, is chosen to zoom in on the zero of highest interest.

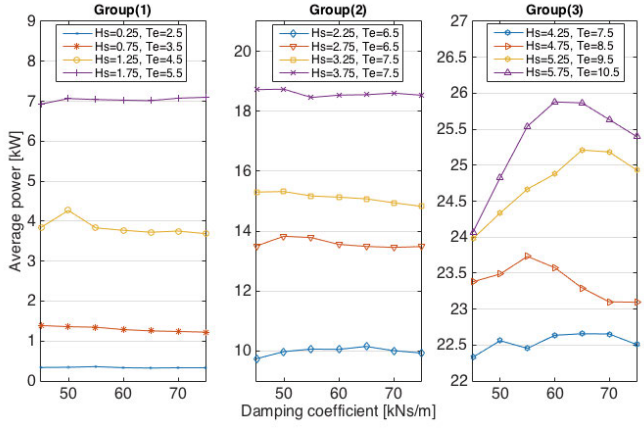

Figure 5.2. Grouped power profiles with damping coefficients from 45 kNs/m to 75 kNs/m.

A comparison between and within the three groups can be seen in Figure 5.2. The maximum power points in both Group (1) and Group (2) are not as obvious as those in Group (3). In Group (3), the optimal damping coefficient greatly influences the power production, and the effect increases with increasingly powerful sea states. Furthermore, it can be observed that for linear damping the optimal damping coefficient is positioned around 60 kNs/m in Group (3), as opposed to 50 kNs/m in Group (1) and Group (2). More details can be found in PAPER V.

5.2 Sea state dependent power production

In line with the results in Section 5.1, a damping coefficient of 60 kNs/m was chosen as the optimal damping coefficient for the following study. It was used to model all the sea states occurring at Test Site 6. A power distribution matrix of the results is shown in Figure 5.3.

In the figure, each value displayed in a square presents the power production in response to a specific sea state. The color bar shows that higher levels of the sea state lead to a higher power production. It should be noticed that the maximum annual energy production is obtained at an energy period of around 5s, when the responding significant wave height is beneath 1.75m, see below.

According to the power matrix in Figure 5.3, the annual energy production can be obtained by knowing the annual occurrence of sea states at a test site. The energy distribution for each sea state is displayed in Figure 5.4.

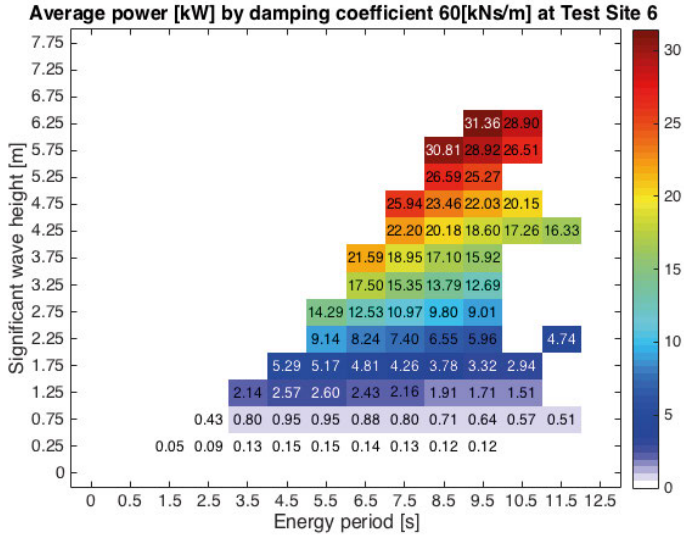

Figure 5.3. The power matrix for the wave climates at Test Site 6 with a constant damping coefficient of 60 kNs/m.

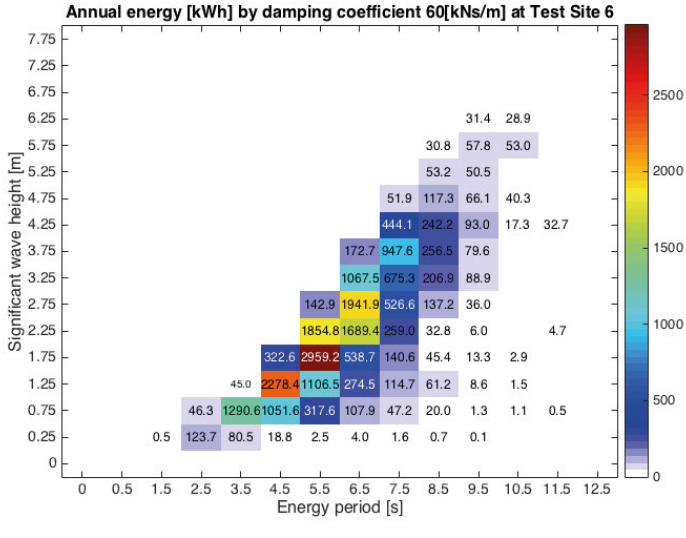

Figure 5.4. The annual energy production for each wave climate at Test Site 6 with a constant damping coefficient 60 kNs/m.

The total annual energy absorption at the studied site is 22.57 MWh. In Figure 5.4, the maximum energy production is found at the wave climate [5.5s, 1.75m], and provides 13.11% of the total production. Even though the power

production is higher at larger sea states, as shown in Figure 5.3, the low occurrence of these sea states makes it so they only provide a small percentage of the overall annual absorption.

6. Impact by Translator Mass

6.1 Comparison between translator weights

In the model, the translator mass was set to 2500 kg, 5000 kg and 10000 kg respectively. A power profile for each mass was generated in relation to a damping coefficient ranging from 5 kNs/m to 190 kNs/m, as presented by the results in Figure 6.1.

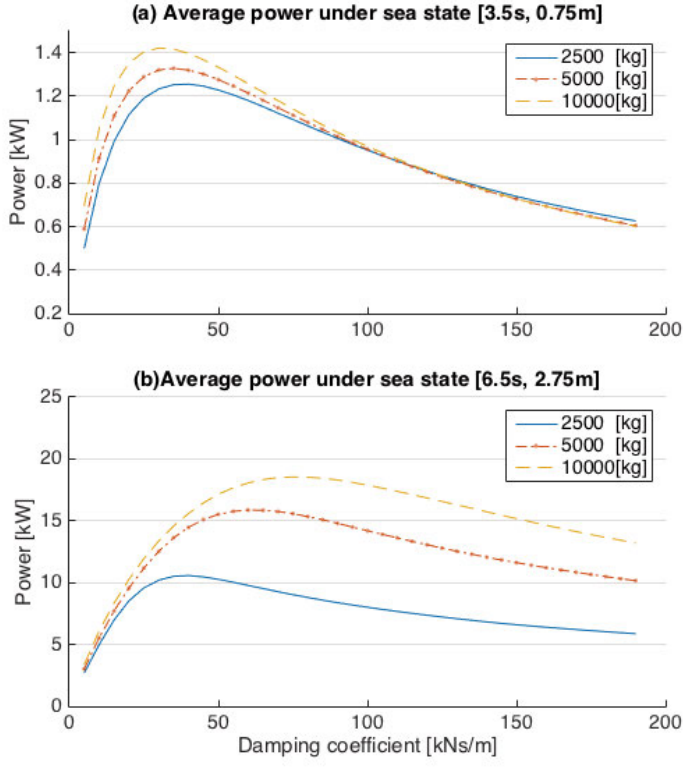

Figure 6.1. Comparison between three translator masses by varying the value of the damping coefficient: (a) under the wave climate [3.5s, 0.75m]; (b) under the wave climate [6.5s, 2.75m].

The model was run for two different sea states. Figure 6.1(a) shows [Te=3.5s, Hs=0.75m] and Figure 6.1(b) shows [Te=6.5 s, Hs=2.75 m]. The power profiles in Figure 6.1 exhibit a similar pattern. The power production increases

and reaches a maximum power point as the damping coefficient increases. After the maximum power point, the power profile drops slowly.

Differences are observed when comparing the two sea states. In case (a), the 10000kg translator obtains the highest amount of power when the damping coefficient is below 120 kNs/m. However, as the damping coefficient increases to a value over 120 kNs/m, the power profiles for both the 5000 kg and 10000 kg case decreases to slightly lower than that for the 2500kg translator, probably due to the limited excitation force from the wave in combination with weight and damping. For case (b), the linear generator with a 2500 kg translator has the lowest power production of the three. The maximum power is associated with the 10000 kg case. The optimal damping coefficient is shown to increase with increasing translator weight.

Based on the findings presented in Figure 6.1, a further study was carried out on the energy transformation over a duration of 10 minutes with the purpose of investigating how the potential energy stored in the translator mass is converted during the translator's descent.

The mechanical force on the translator, as presented in Equation (2.6), is simplified as below,

$$m_b\ddot{x}_2 = f_{line} + f_{damp} - m_b g + f_{upp\_es} + f_{low\_es} \tag{6.1}$$

The energy transformation, in accordance with the conservation of energy, is shown in Equation (6.2), and further simplified in Equation (6.3).

$$\int_0^x m_b\ddot{x}_2 dx = \int_0^x f_{line}\, dx + \int_0^T f_{damp} dt - \int_0^x m_b g dx \tag{6.2}$$

$$\Delta E_p = \Delta W_{line} + \Delta W_{damp} - \Delta E_k \tag{6.3}$$

where W_{damp} is the work done by the damping force and W_{line} is the work done by the force on the buoy line. Note that the energy loss due to friction and heat dissipation is neglected, as well as the energy dissipated from contact with the end stops.

The potential energy stored in the translator, after it has been lifted by a wave, is converted into the three types of energy: kinetic energy, energy consumed by the buoy line, and the damping energy associated with the generation of electricity. The energy consumed in they buoy line (i.e. that which is not converted to kinetic energy or electricity) is energy that is being transmitted back out into the water through the buoy.

In this case, the amount of work done by the line force and damping force is investigated in order to study how much energy that is being transmitted back to the water for different translator masses. Furthermore the study is done to show how much of the stored potential energy that is not converted into useful electrical energy in this case of linear damping.

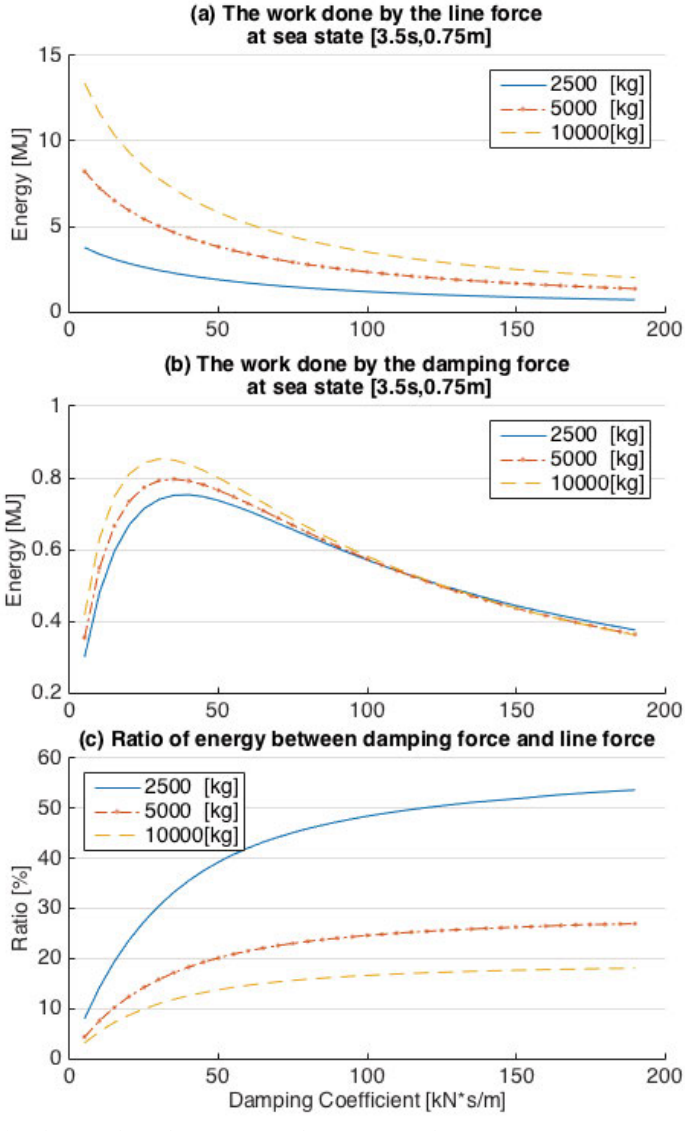

Figure 6.2. The produced energy on the WEC under sea state [3.5 s, 0.75 m], with a variation of damping coefficients from 5 kNs/m to 190 kNs/m: (a) Energy consumed by the buoy line and transmitted back into the ocean through the buoy acting "as a parachute"; (b) energy absorbed by the generator damping and primarily converted into electrical energy; (c) the ratio of energy converted through the line and the generator.

The results are shown in Figure 6.2 and Figure 6.3, respectively, under two different sea states [3.5 s, 0.75 m] and [6.5 s, 2.75 m]. Figure 6.2(a) presents the energy consumed on the buoy line, while 6.2(b) is the energy absorbed by the generator for the less powerful sea state [3.5 s, 0.75 m]. Figure 6.2(c) gives

the ratio of 6.2(a) and 6.2(b). Figure 6.3 gives the same results for the more powerful sea state [6.5 s, 2.75 m].

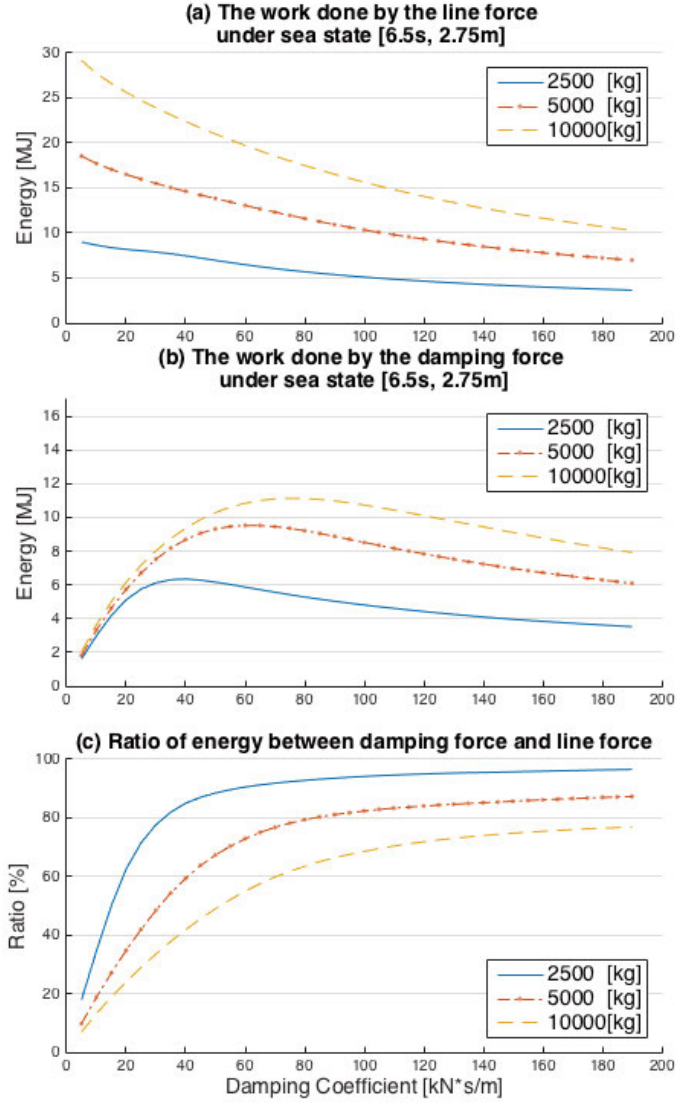

Figure 6.3. The produced energy on the WEC under sea state [6.5 s, 2.75 m], with a variation of damping coefficients from 5 kNs/m to 190 kNs/m: (a) Energy consumed on the buoy line; (b) energy absorbed by the generator damping and primarily converted into electrical energy; (c) the ratio of energy converted through the line and the generator.

In both Figure 6.2 and Figure 6.3, it is clear that a high amount of energy is dissipated through the line force compared with the energy absorbed through the damping force.

A phenomenon is observed: the relative amount of energy consumed on the buoy line decreases as the damping coefficient increases, i.e. more of the absorbed wave energy is converted into useful electrical energy. According to the results for the three studied cases of translator mass, it can be observed that the heavier translators tend to have more energy consumed on the buoy line.

Additionally, as described in Section 5, the optimal damping coefficient shifts with different sea states. Similarly, the optimal damping coefficient differs according to the translator mass. For the sea state of case (a) in Figure 6.1, the optimal damping coefficient does not differ much. On the other hand, the difference is obvious for the three translator weights during the powerful waves of case (b). The optimal damping coefficient tends to be larger as the translator weight increases, but the power production increases as well.

6.2 Power matrix and energy production

By using the recorded wave climates at Test Site 6, power matrices were generated for the three cases of translator weight. The matrices are presented in Figure 6.4. The red lines in case (b) and case (c) are used to visualize the difference between (a), (b) and (c). In case (b), the values above the red line are larger than the corresponding values in case (a). Similarly, in case (c), the values in the part above the red line are larger than the corresponding ones in case (b). The red lines make it easier to observe that most of the sea states in case (b) contribute more power than in case (a). Less than half of the sea states in case (c) produce more power than in case (b).

Table 6.1. The overall annual energy with different translator masses for all the wave climates at Test Site 6.

	Translator Mass [kg]	Annual Energy [MWh]
1	2500	21.62
2	5000	22.57
3	10000	20.84

Power matrices and matrices showing the annual energy are provided in Figure 6.5. The red lines work in the same way as in Figure 6.4. Furthermore, the overall energy production for each case is calculated and listed in Table 6.1. It is interesting to notice that case (b) has the highest overall energy production of the three, even though case (a) has the advantage of having the highest energy production at the sea state of highest occurrence.

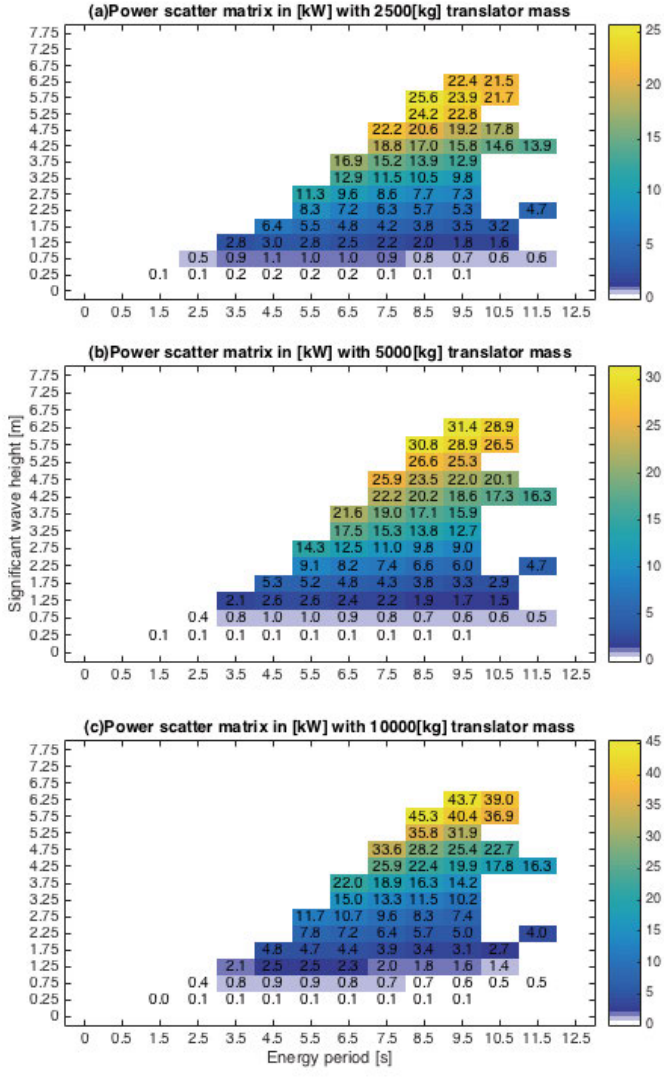

Figure 6.4. Power matrices for three different translator masses under the wave climate at Test Site 6. (a) 2500 kg; (b) 5000 kg; (c) 10000 kg. The power production in the matrices are obtained with a constant damping coefficient of 60 kNs/m and a 4m stroke length.

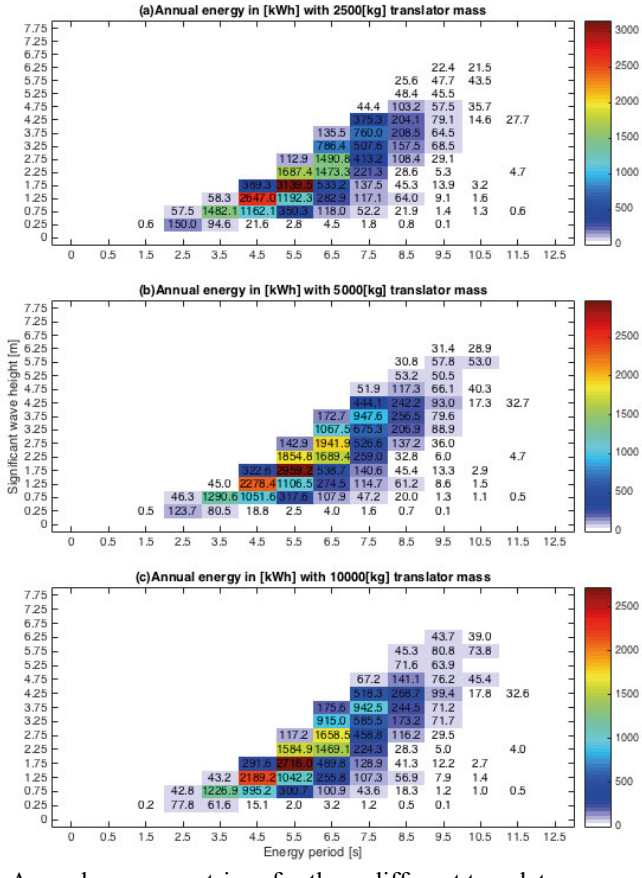

Figure 6.5. Annual energy matrices for three different translator masses under the wave climate at Test Site 6. (a) 2500 kg; (b) 5000 kg; (c) 10000 kg. The energy production in the matrices are obtained with a constant damping coefficient of 60 kNs/m and a 4m stroke length.

7. Influence of Stroke Length

7.1 Concept of stroke length

The stroke length is the vertical distance between the end stop and the translator. It allows the displacement of the translator so it can react with the stator. The stroke length plays an important role in the WEC performance and has a direct effect on how much electrical energy that can be produced from the waves by physically adjusting the translator's available displacement. In an idealized case with an infinite stroke length, the electrical energy from the waves would be converted fully, without any restriction on the translator's movement and regardless of the boundary constraint by the stator. In reality however, neither the generator stroke nor the stator can be made infinitely long. Because of this, one challenge is that the translator will hit the upper and lower part of the WEC structure during large waves, which has an impact on survivability and design requirements. Another challenge is that it is necessary to balance the energy production with the high cost of building a generator, e.g. by effective use of the stroke length. Hence it is necessary to study and determine an optimized length for the translator's displacement so as to understand the consequences both in terms of survivability, energy absorption and production cost in different wave climates.

7.2 Consequences of a limited stroke length

The 2 m, 4 m and infinite stroke length were chosen as case studies, according to the wave climates recorded at the test site. Figure 7.1 gives the results of the generator's performance under an identical irregular wave (9.5 s, 6.25 m), with three different settings of for the stroke length. The vertical axis is the movement of the translator's central point, corresponding to a time domain of 600 s.

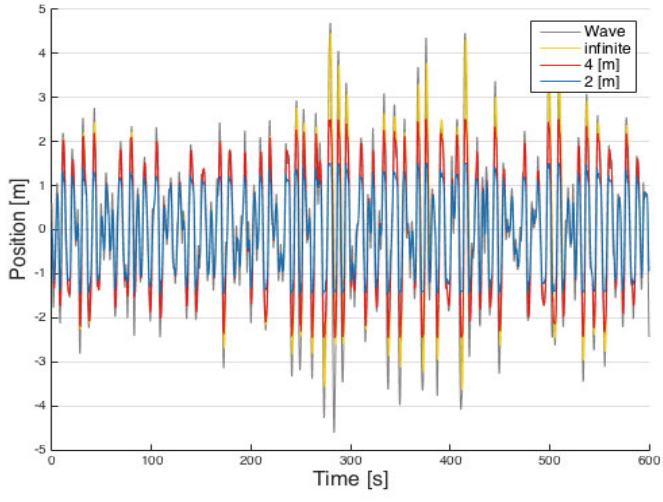

Figure7.1. Translator displacement with three different stroke lengths under one identical wave climate.

It can be observed in Figure 7.1 that the translator with an infinite stroke length follows the waves very well, while the stroke length of 2m and 4m both have a constraining effect on the translator's movement, with the effect of reducing the energy absorption.

7.3 Energy production at test sites 6

A power matrix is obtained from limiting the stroke length, as shown in Figure 7.2. In the figure, the upper diagram is the case of the 2 m stroke length, the middle diagram shows the 4m case and the lower diagram shows the case without a constraint by the stroke length on the translator's motion. The values represent the average power during one hour at the corresponding sea state. The following observations can be made about the power matrices: i) The average power is enhanced as the significant wave height increases. This is expected and is explained by the higher excitation force brought by the more energetic waves; ii) For identical significant wave heights the average power generally decreases as the energy period becomes longer. The average energy absorption is clearly confined by the limits of the stroke length, as seen in (a) and (b).

When comparing the power matrices of case (a) and case (b), a boundary can be observed that relates to the differences in stroke length. The boundary is marked with a red line in Figure 7.2(b) for the benefit of the reader. The values in the lower part of the diagram (b) matrix have identical values as in

Figure 7.2(a). However, the values in the upper part of Figure 7.2(b) are significantly higher than those in Figure 7.2(a).

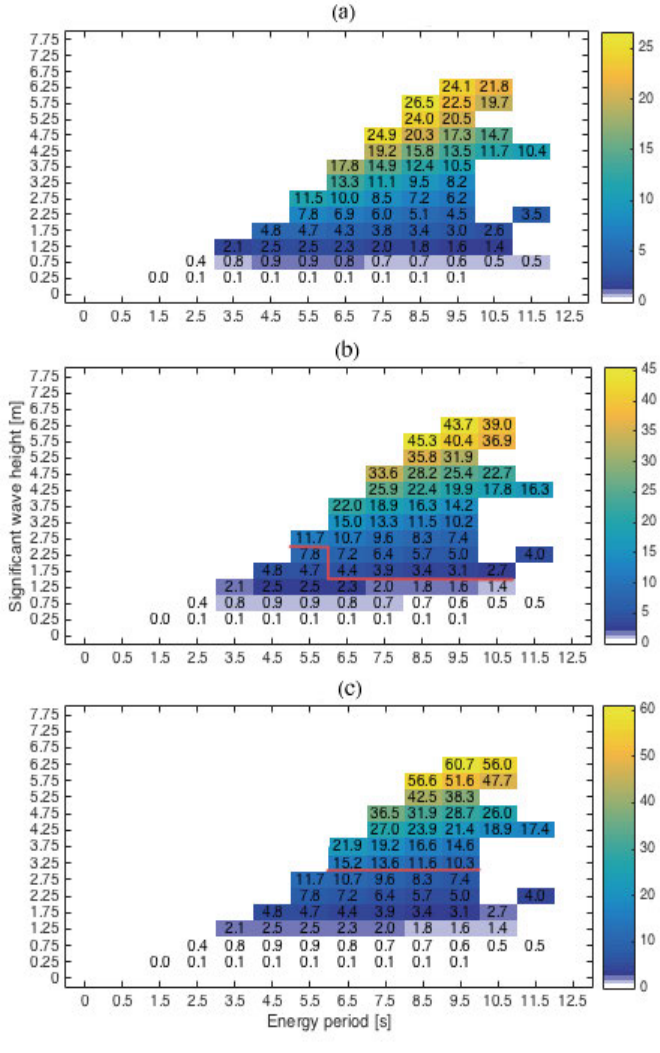

Figure 7.2. Power matrices for three different stroke-lengths. (a) 2 m stroke length; (b) 4 m stroke length; (c) infinite stroke length. The power production in the matrices is obtained by a constant damping coefficient of 60 kNs/m and a translator mass of 10000 kg. The red line marks the difference to the preceding power matrix.

Similarly, there is a red boundary line in Figure 7.2(c). This line distinguishes the power production in case (b) from case (c). Here it can be observed that the values in the upper part of the matrix are higher for case (c) while the values in lower part are the same.

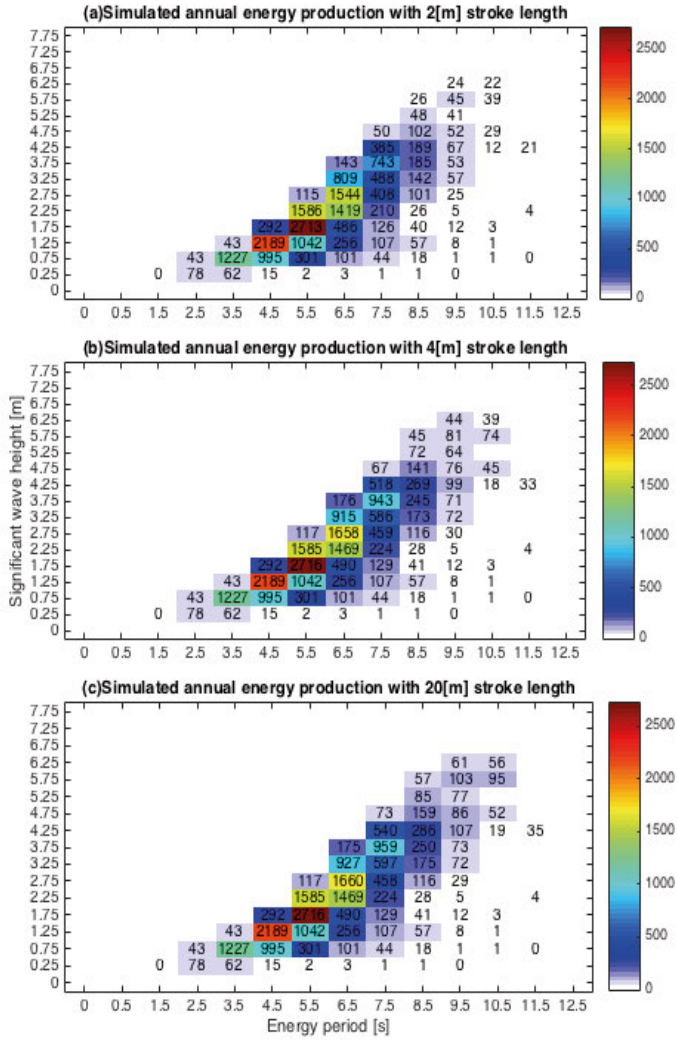

Figure 7.3. Annual energy matrices for three different stroke-lengths under the sea states occurring in Test Site 6. (a) 2 m stroke length; (b) 4 m stroke length; (c) infinite stroke length. The power matrices are obtained with a constant damping coefficient of 60 kNs/m and a translator mass of 10000 kg.

Figure 7.3 provides the annual energy matrix by using the annual occurrence of the sea states at Test Site 6. A comparison is made by calculating the annual energy using different cases of the stroke length.

Table 7.1. Overall annual energy with three cases of stroke length at Test Site 6.

	Stroke Length [m]	Annual Energy [MWh]
1	2	19.48
2	4	20.84
3	Free of limitation	21.10

8. Discussion

Although most of the results are presented in the previous chapters, an explanation of the whole work is necessary, in order to provide a comprehensive view of this study. The study focuses on building a linear generator model and on using the model in the Lysekil case.

8.1 Reviews of control strategies and the Lysekil project

During the earliest part of the thesis work a review was published on electrical strategies suggested for the control of WECs and higher energy production, see Paper I. In this study, the WECs were classified into three types with regards to their mechanical construction: the oscillating water column, the overtopping device and the attenuators. The electrical control strategies were studied according to these categories. The purpose of this review was to give a clear picture of which control methods that are commonly used for the WECs.

Updates on all of the ongoing multidisciplinary research topics in the Lysekil Project are presented in Paper II and III. The review shows the significance of this WEC project in contributing knowledge and experience to the wave energy research field. Furthermore, this knowledge could provide a chance to seek cooperation between different WEC projects.

8.2 The linear generator model

The development of the numeric WEC model used in this thesis is based on the Lysekil Project WEC concept, and further validated by the test results from the WECs installed offshore, see Paper IV. The results show that the overall phase voltage obtained from the simulations match quite well with the experimental results from the L9.

An overall error analysis on the model is made accordingly, as shown in Figure 8.1 and Table 8.1. The errors could be classified as two types: one type are the errors occurring when the translator is at zero displacement; another type are the errors occurring when the translator's speed is at 0 m/s. Figure 8.1(a) gives the difference between the experimental and simulated phase voltage within 5 seconds, which is based on Figure 4.2(c). Note that a high error

difference occurred at 46.5s when the translator is at 0 m/s. Figure 8.1(b) presents a comparison between the experimental and simulated instantaneous power, in order to investigate the impact of this error on the generated power. It can be observed that although the impact is high for the instantaneous power the error over one minute of time is only 2.33% which calculated by Equation (8.1), or a standard deviation of 0.46 kW. The error levels might be possible to improve with better calibration at the zero crossings of both the velocity and the position of the translator.

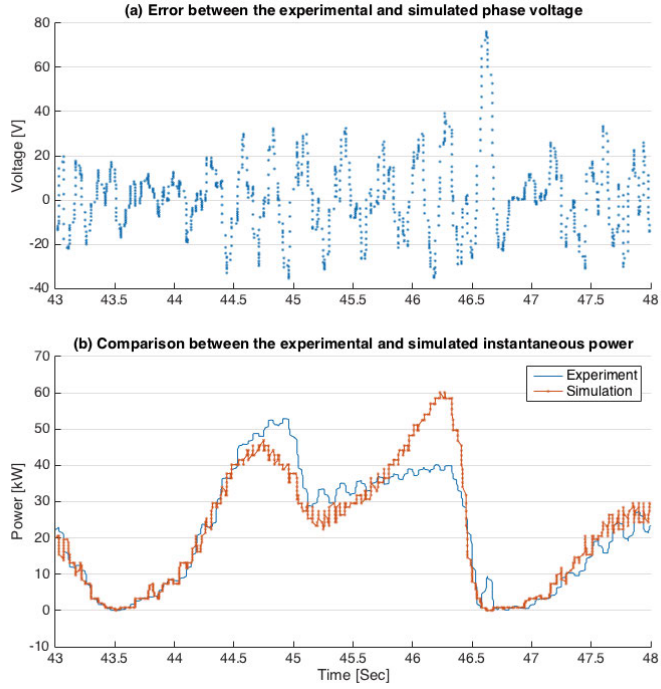

Figure 8.1. Error analysis of the linear generator model. (a) Difference between the experimental and simulated results; (b) Comparison between the experimental and simulated instantaneous power.

$$Error\ Rate = \frac{P_{exp} - P_{sim}}{P_{exp}} \times 100\% \quad (8.1)$$

Table 8.1. Error analysis of the linear generator model with experimental results.

Analysis	Value
Simulated average power [kW]	19.06
Experimental average power [kW]	19.51
Percentage error on the average power[%]	2.33
Standard deviation on average power [kW]	0.46
Standard deviation on phase voltage [V]	16.41

After the validation, the model was connected to a series of electrical load systems. The load strategies used in the simulations are all based on real experiments performed in the Lysekil Project. The WEC model can be used as a platform for the advanced studies on the performance of a direct-drive WEC device with a wide range of different design parameters. However, the WEC model could also be improved so as to be able to provide simulated results, e.g. including electrical and mechanical losses. In modelling, the function for calculating the losses is complicated, some elements including mechanical friction, losses in electrical transmission, eddy current losses and losses associated with magnetic materials.

It is important to clarify that there are always uncertainties associated with simulations. A minor mistake in programming can easily lead to unrealistic results, and this becomes more sensitive the more complicated the real case is. This is the basic reason why experiments, conducted in order to validate the theory, are so vital to research.

8.3 Optimal damping coefficient

8.3.1 Impact on power production

Optimal damping is a key to enhancing the energy absorption for a direct-drive WEC model, see Paper V. In the study, twelve different sea states are used to investigate the power production by varying the damping coefficient. The results show that each power profile has a maximum power point corresponding to an optimal damping. Due to the random phase derived in the irregular waves, the curves are not as smooth as expected with harmonic wave sources. However, this situation would be improved by using more samples in the modelling. Table 8.2 lists the maximum power for each wave case with a corresponding optimal damping coefficient, in addition to the power capture ratio.

Power profiles under powerful sea states are more sensitive to the damping coefficient compared to weaker sea states. The corresponding optimal damping factors under powerful waves are more likely to be gathered in a narrow span. The results thus suggest that controlling the optimal damping is useful for gaining higher energy absorption under powerful wave conditions. Possibly due to the lower excitation forces from the waves, the optimal damping under milder sea states is not as apparent. However, this does not mean that a damping control is not necessary since real wave climates include both mild and powerful sea states. Therefore, a control technique is useful, either to control forces from large waves or for the purpose of enhancing energy production. For cases with gentle wave climates, the corresponding optimal damping suggests a lower threshold for the damping control.

Table 8.2. A list of the optimal damping coefficients and relevant average power for each sea state.

Translator Weight = 5000 [kg]					
Wave Height [m]	Wave Period [sec]	Optimal Damping Coefficient [kNs/m]	Average Power Corresponding to the Optimal Damping [kW]	Available Captured Power [kW]	Power Capture Ratio [%]
0.25	2.50	25.00	0.12	0.15	80.00%
0.75	3.50	35.00	1.42	1.93	73.58%
1.25	4.50	45.00	3.84	6.89	55.73%
1.75	5.50	75.00	7.10	16.51	43.01%
2.25	6.50	65.00	10.15	32.24	31.48%
2.75	6.50	55.00	13.78	48.17	28.61%
3.25	7.50	45.00	15.30	77.63	19.71%
3.75	7.50	45.00	18.81	103.36	18.20%
4.25	7.50	65.00	22.70	132.76	17.10%
4.75	8.50	55.00	23.60	187.95	12.56%
5.25	9.50	65.00	25.21	256.61	9.82%
5.75	10.50	65.00	25.87	340.21	7.60%

8.3.2 Shift of optimal damping

It is interesting to note that the optimal damping coefficient shifts as the wave climate changes, as listed in Table 8.2. The corresponding optimal damping increases as the waves become higher. This phenomenon shows that lower damping is needed to obtain maximum power production for a milder sea states. The relatively narrow band of optimal damping and the shape of the power profiles for milder sea states suggests that controlling the damping could be limited to a small range, or possibly even a specific value, as long as this value can balance the optimal damping between powerful and mild sea states – with the goal of maximizing the annual energy production.

8.3.3 Energy production

This study generated a method of power matrix, in order to display the power distribution during all occurring wave climates within one specific area. Similarly, an annual energy matrix was generated. As shown by the colour-bar used in the matrices, the highest energy production is actually not in an area with powerful wave climates. This phenomenon is due to where the highest annual occurrence for the sea states, as illustrated in Figure 8.2.

Table 8.3 gives a list of the most important sea states from an annual energy perspective. The results tell that sea states with wave heights between 0.75m to 2.75m and wave periods from 3.5s to 6.5s are contributing almost 54% of the overall energy production. This gives important suggestions for designing a WEC, i.e. the stroke length, and a damping control strategy.

Table 8.3. The sea states with the highest contribution to the annual energy at Test Site 6.

Order	Wave Period [s]	Wave Height [m]	Annual Energy Production [MWh]	Percentage [%]
1	5.50	1.75	2.96	13.11
2	4.50	1.25	2.28	10.10
3	6.50	2.75	1.94	8.61
4	5.50	2.25	1.85	8.22
5	6.50	2.25	1.69	7.49
6	3.50	2.75	1.29	5.72

To be noted, the performed study is based on constant damping coefficients. In reality, however, even for the case with a linear resistive electrical load, the damping coefficient is not exactly constant. This is due to several reasons such as the varying active area of the stator, and the inductances and capacitances of the coils and sea cables. For simulation purposes, however, it is much convenient to make comparison among different cases. Besides, it gives valuable reference on further study on control strategies to optimize the energy absorption. A constant coefficient, should it be desired in real experiments, could be achieved with active load control.

8.4 Impact by varying the mechanic designs

8.4.1 Translator mass

The translator mass along with the sea state has a significant impact on the generator's power production. The results show that the power production can be enhanced with a heavier translator mass.

Our studies show that for heavier weights, as presented in Figure 6.2(c) and 6.3(c), a large amount of the absorbed energy is dissipated by the line force. This means that instead of being transformed into electrical energy by the generator damping force it is sent back out into the ocean. Intuitively one can view the buoy as acting like a parachute during the translator's descent. For the lighter weights, such as the 2500kg case, the ratio of the damping energy to the buoy line energy is higher meaning that, although the power production is lower than for then heavier translators, a larger portion of the absorbed energy is converted into useful electrical energy. The results for all translator masses, in particular the heavier ones, suggest a much higher potential for electrical power production, likely to be achieved through the implementation of active control strategies.

In 6.1 (a) it is interesting to notice that when the damping coefficient reaches above 120 kNs/m, the work by damping with a 10000 kg translator is lower than that with a 5000 kg translator. The reason could be that the excitation from the waves is insufficient to drive the heavy translator to overcome

the high inertia of the system, i.e. not enough translator motion is induced. Furthermore, the small size of the buoy is related to the excitation force and is thus a reason for the insufficient energy absorption from the waves.

As illustrated by the results given in Figure 6.3, when the generator performs under a more powerful sea state such as [6.5 s, 2.75 m], a lighter translator (2500 kg) fails to absorb as much energy as a heavier translator (10000 kg). Due to the principle of operation of the studied WEC technology, potential energy is transferred to the translator when lifted by the waves. This potential energy is all that is available for energy production during the translator's descent. Thus, it is important to consider the weight of the translator when designing a WEC for a specific wave climate.

Another interesting result is that after the maximum power is reached, a clear downward trend is observed. The reason is that the translator's movement is affected inversely if the damping force increases to a level where the excitation force fails to drive the translator. On the positive side, a high damping coefficient could also be used to prevent mechanical harm from large waves by decreasing the translator's speed and avoiding hitting the end stop at high speeds. This could be purposefully achieved through advanced control techniques where monitoring and control of the damping coefficient is applied in order to limit the translator stroke to a safe working zone.

Furthermore, our findings show that a light translator can cause spikes in the line force when the power production is at or near its maximum point. This is due to the increased risk of snap loads. For example, if the translator has been pulled to a high position but fails to fall through the stator with the same speed as the buoy is descending then there will be a slack in the line between buoy and translator. When the buoy starts moving upwards again, while the translator is still moving downwards, the sudden tightening of the rope will cause a snap associated with a high momentary force which can cause harm to the device.

A heavier translator stores a higher amount of potential energy that can be harnessed as it moves downwards during half of a wave period. If the translator is too light and the damping high, then the buoy will move down in wave troughs at a higher speed than the translator moving through the stator. The translator will not make it all the way through the stator before the buoy pulls it upwards again. This will lead to an inefficient use of the generator and therefore lower energy absorption. If the translator is very heavy, less powerful sea states may not be able to make the translator move much, but the results indicate that this is not as significant, at least not for the studied weights. The results of the study show that, for translators weighing 2500 kg to 10000 kg, the energy absorption increases with higher weight, particularly under the conditions of more powerful sea states.

8.4.2 Stroke length

The stroke length more or less affects the linear generator's performance by limiting the behaviour of the translator, see Paper VI. The focus on the stroke length is to estimate how much impact it would have on the energy production of the direct-drive WEC device. Three cases of stroke length are investigated by simulating a prototype WEC from the Lysekil project under different wave environments.

The impact of the stroke length on the power production is strongly wave climate dependent, i.e. a longer stroke length would surely contribute to higher energy absorption. However, by studying the wave climate of a particular site some indication is given for the design of the stroke length. Taking the studied site 6 on the Swedish west coast as an example, the energy production between a 4m stroke length and an infinite stroke length differs little. So there seems to be a strong economic incentive to limit the stroke length. In other words, a good design for the stroke length is one that is able to balance both the economic benefits and the technical benefits. The results suggest that a 2m stroke length is sufficient for Sweden, while a longer stroke length has more benefits at test sites which contain more wave energy, such as the offshore locations studied in Scotland and Chile.

Table 8.4. The annual energy absorption at different translator mass for all the wave climates occurring at Site 6.

Overall Annual Energy [MWh]			
Translator Mass [kg] / Stroke Length [m]	2500	5000	10000
2	20.47	20.95	19.48
4	21.62	22.57	20.84
Free of Limitation	21.67	23.00	21.10

The translator mass also plays an important role in designing the stroke length. Table 8.4 shows a relationship between the stroke length and the translator mass. Each overall annual energy for Site 6 is obtained based on the corresponding stroke length and translator mass in the table. It is obvious that the weight of the translator and the stroke length both have an effect on the energy production. Aside from the case with unlimited stroke length, the highest energy production was obtained with the 5000 kg translator and a 4 m stroke length.

9. Conclusions

The most significant conclusions drawn from this thesis work as follows:

a. It has been verified that the linear generator model, including the hydrodynamic driving forces and electrical loads, agrees with the experimental results from the WEC prototype in the Lysekil project. (Paper IV)

b. The optimal linear damping for the studied direct-drive WEC device has been described in detail, with results that can be used to increase the energy absorption. The optimal damping is wave climate dependent, i.e. the optimal damping shifts as the wave climate changes. Results suggest the optimal damping coefficient tends to increase as the wave climate becomes stronger. For the Lysekil case, 60 kNs/m is a good compromise to accommodate all the different sea states documented at the test site. (Paper V)

c. The translator mass plays a significant role in the WEC's performance. From the results, it can be concluded that linear generators with a heavy translator (up to the studied 10000 kg) can enhance the power and energy production. (Paper V)

d. A longer stroke length contributes to more energy production in a direct-drive WEC device. However, the wave climate at the test site should be taken into account as an important factor when designing the length. The design should aim to find a compromise between the construction cost and the gain to the energy production. Results from the numeric modelling suggest that a 2 m stroke length is sufficient for the Lysekil Project. (Paper VI)

e. The translator mass and the stroke length have a combined effect on the energy production for a direct-drive WEC. For the wave climate in Test Site 6, a combination of a 4 m stroke length and a 5000 kg translator is suggested as optimal to obtain a higher energy production. However, a larger buoy together with a heavier translator is likely to increase the energy production even further.

f. Power matrices and annual energy absorption matrices for Uppsala University prototype WEC (L9) have been provided. The matrices have been used to indicate optimal design parameters for the WEC devices, both in terms of mechanics (stroke length and translator mass) and load strategies (energy absorption).

10. Future Work

Although the direct-drive WEC model is validated by test results, more improvements can be made to optimize the simulations to a level where the model can perform even more realistic simulations. One challenge to this purpose is to incorporate losses in the WEC model. Therefore, a thorough study of the losses in experiments would be an important step towards updating the WEC model.

The optimal damping studies in this thesis have been focused on linear damping. There are many other types of damping suggested in the literature, out of which active control is of particular interest for the Uppsala university technology. A natural next step is to study this more thoroughly in theory, simulations and experiments.

Since the cost of constructing and maintaining a WEC is of paramount importance for the long term viability of the technology, a financial model that takes into account the construction cost and the various engineering decisions outlined in this thesis (e.g. translator stroke length and mass) would be of great value. It is envisioned that such a model should be developed.

The power matrix for the L9 allows for studies of energy production should the WEC be placed in other locations internationally. Power matrices for more modern versions of the WEC technology would also be interesting to study and to apply to wave climates around the world, and in combination with a financial model.

11. Summary of Papers

All the papers included in this thesis deal with wave energy in one way or another. Paper I, categorizes the WEC devices based on the devices' electrical control methods. Paper II and III present a status update of the Lysekil Project from 2011 to 2015. Paper IV proposes a numerical linear generator model which is verified by the test results. Paper V describes the study of how the damping coefficients affect the performance of the linear generator while Paper VI focuses on the impact of the generator stroke length on the energy production of the direct-drive WEC device.

PAPER I

Review on Electrical Control Strategies for Wave Energy Converting Systems

In this paper, different types of wave energy converters are classified by their mechanical structure and by the way they absorb energy from ocean waves. The paper presents a review of the strategies for electrical control of wave energy converters as well as energy storage techniques.

The author performed most of the work including reviewing literatures and writing work.

Published in *Renewable and Sustainable Energy Reviews*, 31:329–342, 2014.

PAPER II

Status Update of the Wave Energy Research at Uppsala University

The paper gives an updated review on the researches happening within the Lysekil Project. The presented material includes both theoretical and experimental research developments, such as new designs and installations of generators, experimental results of rectification on power production as well as further developments in the experimental setup at Lysekil. The paper also presents research on a device for avoiding tidal effects and environmental studies by Uppsala University.

The author was responsible for organizing and writing all the info from co-authors into one complete paper.

Presented by the author at the *Proceedings of the 10th European Wave and Tidal Energy Conference*, Aalborg, Danmark, 2-5 September, AWTEC 2013

PAPER III

Wave Energy Research at Uppsala University and The Lysekil Research Site, Sweden: A Status Update

The paper provides a status update of the Lysekil wave power project from 2013 up till 2015. In the paper, progress on different research topics are presented during these two years.

The author contributed one sub-section to the article on the design of the linear generator model.

Presented by Arvind Parwal at the *Proceedings of the 11th European Wave and Tidal Energy Conference*, Nantes, France, 6-11 September, EWTEC2015

PAPER IV

Linear Generator-based Wave Energy Converter Model with Experimental Verification and Three Loading Strategies

In this paper a WEC model is proposed.

The paper focuses on analyzing the operation of the model coupled to the three load cases. The results verify that the WEC model simulates the linear generator developed in the Lysekil Project correctly.

The results give an indication on the efficiency of the energy production as well as on the force ripples and resulting mechanical loads on the wave energy converters.

The author was responsible for the modelling results and wrote most part of the article.

Published in *IET Renewable Power Generation*, 10(3): 349-359, 2015

PAPER V

A Study on the Damping Coefficient of a Direct-drive Type Wave Energy Converter

The study gives an investigation of the mass of the generator's translator with the purpose of quantifying the impact of the translator's mass on the power production. The impact of the linear damping on the power production is also studied for different wave climates along with the potential annual energy absorption under the given conditions.

The author ran the simulation and was responsible for all the results. She wrote most of the article.

Conditionally accepted in *Renewable Energy*, September, 2016

PAPER VI

Impact of Generator Stroke Length on Energy Production for a Direct Drive Wave Energy Converter

This paper studies the impact of the generator stroke length on energy absorption for three sites off the coasts of Sweden, Chile and Scotland. 2 m, 4 m and unlimited stroke are considered. Power matrices for the studied WEC prototype are presented for each of the studied stroke lengths.

The author built up the modelling and was responsible for all the results. She wrote most of the article.

Published in *Energies,* 9: 730-742, 2016

12. Svensk Sammanfattning

Havsvågor, som täcker två tredjedelar av jordens yta, har en enorm potential som en källa till förnybar energi. Det skulle därför vara en enorm prestation om tekniska innovationer lyckas omvandla energin till en form som kan användas framgångsrikt av samhället. I åratal har forskare och ingenjörer försökt göra detta genom att utveckla vågkraftverk av många olika slag med syfte att omvandla vågenergin till elektrisk energi.

I denna avhandling studeras en vågkraftteknik som är utvecklad på avdelningen för elektricitetslära vid Uppsala universitet, inom det så kallade Lysekilsprojektet. Lysekilsprojektet startade 2002 och har en experimentanläggning på västkusten i närheten av Härmanö och Lysekil. Hittills har mer än tio prototyper av vågkraftverk tagits i bruk och en stor mängd experiment har utförts i experimentanläggningen.

Den typ av vågkraftverk som utvecklats vid Uppsala universitet kategoriseras som en punktabsorbator. Den består av en direktdriven linjärgenerator som är kopplad till en flytande boj. Linjärgeneratorn står på havsbotten och kopplas via en lina eller vajer till den av havsvågorna drivna bojen på ytan. I generatorn omvandlas bojens rörelser till elektrisk energi, och den producerade elen överförs till en mätstation på land.

Arbetet som presenteras i denna avhandling behandlar dels ett simuleringsverktyg för att som bland annat beräknar hur mycket energi som vågkraftverken absorberar beroende på en rad faktorer – bland annat vågklimat, kontrollmetoder för generatorns dämpning, och mekaniska parametrar så som massa och slaglängd hos linjärgeneratorn. Syftet är att optimera energiabsorption och samtidigt ta hänsyn till de konsekvenser detta har på både ekonomi (att bygga och underhålla vågkraftverken) och mekanisk prestanda (att kraftverken överlever de stormar till havs). Två mekaniska egenskaper hos linjärgeneratorerna studeras i större detalj – deras slaglängd och vikt. Syftet är att hitta en rimlig konstruktion för generatorn som balanserar tillverkningskostnaden och energiproduktionen.

De erhållna resultaten visar att det vid linjär dämpning går att finna en dämpkonstant som är en tillräckligt bra kompromiss för att användas vid alla Svenska vågklimat – och därigenom förenkla kontrollen av vågkraftverken.

Resultaten presenterar även matriser som beskriver den studerade vågkraft-prototypens energiabsorption vid alla olika vågklimat, vilket gör det möjligt att förutsäga energiabsorptionen oavsett var i världen som vågkraftverket hade varit placerat.

13. Acknowledgement

With my sincere gratitude, I am now writing this last piece for my thesis at my office 11205 in Ångströmlab, and trying to recall all my memories for these five years. As a very shy girl, I had never imagined a life in a foreign country 5 years ago until I arrived in Sweden with my first step. Sweden brings me wholly fresh experience, which I never had in China, just feeling like my second home country.

Therefore, I want to express my sincere thanks to Mats Leijon firstly, who gave me this opportunity to experience the student life in Sweden. As I remembered the first day I arrived, our wave group was having a regular meeting (held by Cecilia and Magnus). In that meeting, Mats told me: 'Life is like an elevator, if you don't keep walking up, then you will fall behind.' I thought I understood it quite well, but actually it took me 5 years to get this meaning. And also great thanks to the CSC project, supporting my studies and living for four years in Sweden.

I would like to send my highest gratitude to Rafael Waters, my main supervisor who has been spending a lot of energy on me and my research, and has been providing me with his best support. I think I did worry him a lot on my research. Besides, he sets up a very good example as the leadership for a research group. Also through these years, I start to have a clue on how to supervise a PhD student, and this will never be an easy job.

Mikael Eriksson, my co-supervisor, great thanks for your support and teaching on hydrodynamics. I shall say I won't have the confidence to continue with my research without your help. Besides, thanks to Mikael, I learn the spirit of being a researcher.

Lots of thanks to Cecilia Boström, one of my co-supervisors as well, always supports me friendly with very useful advices.

Janaina G.O., Juan S., Marcus B., Fredrik B., Johan A., Simon M., Boel, E. Thank you so much for your kindness and lots of help when I started my PhD life.

Jon O., being my first roommate at 11205 for almost three years, thanks a lot for so many opportunities to listen to your concerts. Your performance is so wonderful and joyful.

Morgan R., my second roommate for over one year, thanks a lot for helping me with the Latex, and your sincere attitude on both teaching and research really inspires me. And thanks for helping me to report the first raccoon I saw in Sweden.

Magnus H. Thanks for the good memories on the course we took in KTH, and also thanks for your warm help on learning Matlab as well as the lab course.

Olle S. Thanks for sharing your music albums, and inviting me to watch your performance in the theater. it's so lucky to meet you and I like your musical spirit! Never forget 'Smoke on the water' you played in your dissertation party.

Linnea S. and Stefan S., thanks for telling me about all the Swedish traditions you know, and thanks for the good memories on the party for your new home.

Valeria C., thanks for our happy memories in Japan and your precious help in my research project.

Johan F. thanks for your warm heart and encouragement, and also our happy memories in Japan with Valeria C. and Ling H.

Maria A. What a pleasure having you as my good friend, I enjoyed a lot during our trip in Denmark and San Francisco together.

Minh Thao G. thanks for the wonderful trip in Greece. Hopefully we will have another trip together with Maria A. in the future, as we have been discussing about it for long.

Liselotte U. A lot thanks for your warm help on correcting my first conference article, and your strong spirit and hard work in Lysekil was very impressed.

Per R. It's so great to meet you and your little Elise, thanks for inviting me to your birthday party, and wonderful memories for organizing the summer party with Linn S. together in 2012!

Kristin B. It's so grateful for proofing my thesis in such limited time, even it occupied your weekend.

Ingrid R., Maria N., Thomas G., and Emma H. Thank you so much for your friendly help.

Wei L., Wei jia Y., Li Guo W., and Hai L. Such a pleasure to meet you and have fun together, I really enjoy our memories at different Chinese restaurants in Uppsala.

Wensong B., Xie L., Weiwei S. Ling H. and Jiangtao C. It's really pleasure to meet you all in Xiaofanzhuo discussing all the things around at the lunchtime, and hiking together on weekends.
And also thanks for Yuanyuan H. and Dan W. I feel so glad and surprised to find out we share such common interests on anime and movie.

Yajun W. and Jing Z., thanks for living together, sharing lots of funny memories together with Swahns. So surprised you guys are now working at my hometown. Hopefully we will meet again there.

My dear Family Swahns: Sabina, Esbjörn, Lisa, Allan, and Rikard. I love you all!!! You bring me such a wonderful life in Sweden with countless precious and special memories. We had meals, played games, and went travelling together. I will never forget the wedding of Allen and Lisa, and also the warmth you brought to me after my surgery in hospital. I feel so proud and thankful to be living with you for over five years, being a member in this family. I'd be very happy to guide you if you have any plan visiting my hometown in the future.

我由衷感谢赵大哥和王姐，很幸运能在瑞典遇到你们。Hikari Sushi 就像是我的心灵港湾，每次去感觉就像回家再次见到了自己家人，无论是“一般一般世界第三”的佳肴，还是每每的畅饮欢谈，都让我倍感温馨。

最后，感激赐予了我生命的父母，在我决定出国时给予了许多支持。尽管我远在他乡，他们也时刻不忘给予我精神关怀。也正是那份遥远的思念，我才懂得了故乡情深。

Bibliography

[1] Y. Masuda. Wave-activated generator. *Int. Colloq Exposition Oceans*. France: Bordeaux; 1971.

[2] Y. Masuda. Experimental full-scale results of wave power machine Kaimei in 1978. *Proceedings of First Symp Wave Energy Utilization*. Gothenburg, Sweden, 349–63, 1979.

[3] M.E. McCormick. Ocean wave energy conversion. *New York: Wiley*, 1981.

[4] T.W. Thorpe. A brief review of wave energy. *Harwell Laboratory*, Energy Technology Support Unit, 1999.

[5] B. Drew, A.R. Plummer, M.N. Sahinkaya. A review of wave energy converter technology. *Proceedings of the Institution of Mechanical Engineers, Part A: Journal of Power and Energy*. 223, 887–902, 2009.

[6] I. López, J. Andreu, S. Ceballos, I. Martínez De Alegría, I. Kortabarria, Review of wave energy technologies and the necessary power-equipment. *Renewable and Sustainable Energy Reviews*. 27 413–434, 2013.

[7] Seabased AB. Wave Energy Converter 2013. Available online: http://www.seabased.com/. Online; accessed 19-Oct-2016.

[8] M. Leijon, O. Danielsson, M. Eriksson, K. Thorburn, H. Bernhoff, J. Isberg, et al., An electrical approach to wave energy conversion. *Renewable Energy*. 31, 1309–1319, 2006.

[9] A.F. de O. Falcão. Wave energy utilization: A review of the technologies. *Renewable and Sustainable Energy Reviews*. 14, 899–918, 2010.

[10] T. V Heath. A review of oscillating water columns. *Philosophical Transactions of the Royal Society A Mathematical Physical and Engineering Sciences*. 370, 235-245, 2011.

[11] R.H. Charlier, J.R. Justus. Ocean energies: environmental, economic and technological aspects of alternative power sources. *Elsevier*. 1993.

[12] Pico OWC wave power plant on the Azores-a late success n.d. http://wavec.org/client/files/AF_Folheto_Maio_ING.pdf/. Online; accessed 19-Oct-2016

[13] A. Muetze, J. G. Vining. Ocean wave energy conversion-a survey. In *Conference Record of the 2006 IEEE Industry Applications Conference Forty-First IAS Annual Meeting*. 3, 1410-1417, 2006.

[14] M. Jasinski, M. Malinowski, M.P. Kazmierkowski, H.C. Sorensen, E. Friis-Madsen, D. Swierczynski. Control of AC/DC/AC Converter for Multi MW Wave Dragon Offshore Energy Conversion System. *IEEE International Symposium on Industrial Electronics*. 2685–2690, 2007

[15] J.P. Kofoed, P. Frigaard, E. Friis-Madsen, H.C. Sørensen. Prototype testing of the wave energy converter wave dragon. *Renewable Energy*. 31, 181–189, 2006.

[16] Wave Dragon. Wave Dragon has started the development of a 1.5MW North Sea Demonstrator n. d. http://www.wavedragon.net/index. php?option=com_content&task=view&id=42&Itemid=67/. Online; accessed 19-Oct-2016

[17] B.M. Count, T. Miyazaki. Hydrodynamic studies on floating attenuator wave energy devices. *Central Electricity Generating Board Technology Planning and Research Division*. 1983

[18] J. Falnes, P. McIver. Surface wave interactions with systems of oscillating bodies and pressure distributions. *Applied Ocean Research*. 7, 225–234, 1985.

[19] K. Budar, J. Falnes. A resonant point absorber of ocean-wave power. *Nature*. 256, 478–9, 1975.

[20] R. Yemm, D. Pizer, C. Retzler, R. Henderson. Pelamis: experience from concept to connection. *Philosophical Transactions of the Royal Society A Mathematical Physical and Engineering Sciences*. 370, 365-380, 2011.

[21] R. Henderson. Design, simulation, and testing of a novel hydraulic power take-off system for the Pelamis wave energy converter. *Renewable Energy*. 31, 271–283, 2006.

[22] Pelamis Wave Power Ltd. The Pelamis absorbs the energy of ocean waves and converts it into clean, green electricity; 2013. http:// www.pelamiswave.com/image-library/. Online; accessed 19-Oct-2016

[23] A. Clément, P. McCullen, A. Falcão, A. Fiorentino, F. Gardner, K. Hammarlund, et al. Wave energy in Europe: current status and perspectives. *Renewable and Sustainable Energy Reviews*. 6, 405–431, 2002.

[24] E. Lejerskog, H. Gravråkmo, A. Savin, E. Strömstedt, S. Tyrberg, K. Haikonen, et al. Lysekil research site, Sweden: A status update. *9th European Wave and Tidal Energy Conference*. Southampton, UK, 2011.

[25] M. Leijon, R. Waters, M. Rahm, O. Svensson, C. Bostrom, E. Stromstedt, et al. Catch the wave to electricity. *IEEE Power and Energy Magazine*. 7, 50–54, 2009.

[26] Uppsala Universitet. Lysekil Project; 2013. http://www.el. angstrom.uu.se/forskningsprojekt/WavePower/Lysekilsprojektet.html/. Online; accessed 19-Oct-2016

[27] M. Leijon, H. Bernhoff, M. Berg, O. Ågren, Economical considerations of renewable electric energy production—especially development of wave energy. *Renewable Energy*. 28, 1201–1209, 2003.

[28] M. Stålberg, R. Waters, M. Eriksson, O. Danielsson, K. Thorburn, H. Bernhoff, and M. Leijon. Full-scale testing of PM linear generator for point absorber WEC. *Proceedings of the 6th European wave and tidal energy conference*, Glasgow, UK, 2005.

[29] A. Parwal, F. Remouit, Y. Hong, F. Francisco, V. Castellucci, L. Hai, L. Ulvgård, W. Li, E. Lejerskog, A. Baudoin, M. Nasir, M. Chatzigiannakou, K. Haikonen, R. Ekström, C. Boström, M. Göteman, R. Waters, O. Svensson , J. Sundberg, M. Rahm, E. Strömstedt, J. Engström, A. Savin and M. Leijon. Wave energy research at Uppsala University and the Lysekil Research Site, Sweden: A status update. *Proceedings of the 11th European Wave and Tidal Energy Conference*, Nantes, France, 2015.

[30] R. Waters, M. Sta□lberg, O. Danielsson, O. Svensson, S. Gustafsson, E. Stro□mstedt, et al. Experimental results from sea trials of an offshore wave energy system. *Applied Physics Letters*. 90, 34105, 2007.

[31] M. Eriksson, R. Waters, O. Svensson, J. Isberg, M. Leijon. Wave power absorption: Experiments in open sea and simulation. *Journal of Applied Physics*. 102, 84910, 2007.

[32] R. Ekström, M. Leijon. Control of offshore marine substation for grid-connection of a wave power farm. *International Journal of Marine Energy*. 5, 24–37, 2014.

[33] M. Rahm, C. Boström, O. Svensson, M. Grabbe, F. Bülow, and M. Leijon. Laboratoty experimental verification of a marine substation. *Proceedings of the 8th European wave and tidal energy conference*. Uppsala, Sweden, 51-58, 2009.

[34] M. Rahm, C. Bostrom, O. Svensson, M. Grabbe, F. Bulow, M. Leijon, Offshore underwater substation for wave energy converter arrays. *IET Renewable Power Generation*. 4, 602–612, 2010.

[35] M. Rahm, O. Svensson, C. Bostrom, R. Waters, M. Leijon, Experimental results from the operation of aggregated wave energy converters. *IET Renewable Power Generation*. 6, 149–160, 2012.

[36] R. Ekström, V. Kurupath, O. Svensson, M. Leijon. Measurement system design and implementation for grid-connected marine substation. *Renewable Energy*. 55, 338–346, 2013.

[37] R. Ekström, A. Baudoin, M. Rahm, M. Leijon. Marine substation design for grid-connection of a research wave power plant on the Swedish West coast. *Proceedings of the 10th European Wave and Tidal Conference*. Aalborg, Denmark, 2013.

[38] R. Ekström, S. Apelfröjd, M. Leijon. Experimental verifications of offshore marine substation for grid-connection of wave energy farm. *Proceedings on the 3rd International Conference on Electric Power and Energy Conversion Systems*. Istanbul, Turkey, 2013.

[39] H. Gravrakmå, M. Leijon, E. Strömstedt, J. Engström, S. Tyrberg, A. Savin, O. Svensson, R. Waters. Description of a tourus shaped buoy for wave energy point absorber. Presented at *the conference Renewable Energy*, Yokohama, Japan ,2011.

[40] H. Gravråkmo, Buoy geometry, size and hydrodynamics for power take off device for point absorber linear wave energy converter, PhD thesis, Uppsala University, 2014.

[41] M. Leijon, C. Boström, O. Danielsson, S. Gustafsson, K. Haikonen, O. Langhamer, et al. Wave energy from the North Sea: Experiences from the Lysekil Research Site. *Surveys in Geophysics*. 29, 221–240, 2008.

[42] C. Boström, E. Lejerskog, M. Stålberg, K. Thorburn and M. Leijon. Experimental results of rectification and filtration from an offshore wave energy converter. *Renewable Energy*. 34(5), 1381-1387, 2009.

[43] C. Bostrom, R. Waters, E. Lejerskog, O. Svensson, M. Stalberg, E. Stromstedt, et al. Study of a wave energy converter connected to a nonlinear load. *IEEE Journal of Oceanic Engineering*. 34, 123–127, 2009.

[44] M. Leijon, C. Boström, B. Ekergård. Electric resonance-rectifier circuit for renewable energy conversion. *PS Public Service Review: European Union*, 22, 268-271, 2011.

[45] C. Boström and M. Leijon. Operation analysis of a wave energy converter under different load conditions. *IET Renewable Power Generation*, 5(3), 245-250, 2011.

[46] A. Baudoin, C. Bostrm, M. Leijon. Thermal rating of a submerged substation for wave power. *IEEE Transactions on Sustainable Energy*, 7, 436–445, 2016.

[47] A. Baudoin, C. Boström. Thermal modelling of a passively cooled inverter for wave power. *IET Renewable Power Generation*, 9(4), 2015.

[48] A. Baudoin, R. Ekström, C. Boström, M. Rahm, O. Svensson, E. Strömstedt, A. Savin, R. Waters, M. Leijon. Temperature study in a marine substation for wave power. *International Journal of Mechanic Systems Engineering*, 2(4), 126-131, 2012.

[49] F. Remouit, M. Lopes, P. Pires, L. Sebastiao. Automation of subsea connections for clusters of wave energy converters. *The Twenty-fifth International Ocean and Polar Engineering Conference*. Kona, Hawaii, USA, 2015.

[50] V. Castellucci, M. Eriksson, R. Waters, S. Ferhatovic and M. Leijon. Wireless system for tidal effect compensation in the Lysekil Research Site. *Proceedings of the ASME 2012 31st International Conference on Ocean*. Offshore and Arctic Engineering, Rio de Janeiro, Brazil, 2012.

[51] V. Castellucci, R. Waters, M. Eriksson, M. Leijon. Tidal effect compensation system for point absorbing wave energy converters. *Renewable Energy*. 51, 247–254, 2013.

[52] O. Langhamer, D. Wilhelmsson. Colonisation of fish and crabs of wave energy foundations ant the effects of manufactured holes – A field experiment. *Marine Environmental Research*. 68(4), 151-157, 2009.

[53] K. Haikonen, J. Sundberg, M. Leijon. Characteristics of the operational noise from full scale wave energy converters in the Lysekil Project: Estimation of potential environmental impacts. *Energies*. 6, 2562–2582, 2013.

[54] O. Langhamer, K. Haikonen, J. Sundberg. Wave power—Sustainable energy or environmentally costly? A review with special emphasis on linear wave energy converters. *Renewable and Sustainable Energy Reviews*. 14, 1329–1335, 2010.

[55] S. Tyrberg, H. Gravråkmo and M. Leijon. Tracking a wave power buoy using a network camera – system analysis and first results. *Proceedings of the 28th International Conference on Offshore Mechanics and Arctic Engineering*. OMAE, Honolulu, USA, 2009.

[56] O. Langhamer, D. Wilhelmsson, J. Engström. Artificial reef effect and fouling impacts on offshore wave power foundations and buoys – a pilot study. *Estuarine, Coastal and Shelf Science*. 82, 426–432, 2009.

[57] K. Thorburn, Electric energy conversion systems: Wave energy and hydropower, PhD thesis, Uppsala University, 2006.

[58] O. Danielsson, Wave energy conversion, linear synchronous permanent magnet generator, PhD thesis, Uppsala University, 2006.

[59] M. Eriksson, Modelling and experimental verification of direct drive wave energy conversion: Buoy-generator dynamics, PhD thesis, Uppsala University, 2007.

[60] R. Waters, Energy from ocean Waves. Full scale experimental verification of a wave energy converter, PhD thesis, Uppsala University, 2008.

[61] O. Langhamer, Wave energy conversion and the marine environment: Colonization patterns and habitat dynamics, PhD thesis, Uppsala University, 2009.

[62] M. Rahm, Ocean wave energy: Underwater substation system for wave energy converters, PhD thesis, Uppsala University, 2010.

[63] S. Lindroth, Buoy and generator interaction with ocean waves, PhD thesis, Uppsala University, 2011.

[64] J. Engström, Hydrodynamic modelling for a point absorbing wave energy converter, PhD thesis, Uppsala University, 2011.

[65] C. Boström, Electrical systems for wave energy conversion, PhD thesis, Uppsala University, 2011.

[66] O. Svensson, Experimental results from the Lysekil wave power research site, PhD thesis, Uppsala University, 2012.

[67] E. Strömstedt, Submerged transmission in wave energy converters:
Full scale In-site experimental measurements, PhD thesis, Uppsala University, 2012.

[68] A. Savin, Experimental measurement of lateral force in a submerged single heaving buoy wave energy converter, PhD thesis, Uppsala University, 2013.

[69] B. Ekergård, Full scale applications of permanent magnet electromagnetic energy converters, PhD thesis, Uppsala University, 2013.

[70] R. Ekström, Offshore marine substation for grid-connection of wave power farms - An experimental approach, PhD thesis, Uppsala University, 2014.

[71] K. Haikonen, Underwater radiated noise from point absorbing wave energy converters: Noise characteristics and possible environmental effects, PhD thesis, Uppsala University, 2014.

[72] R. Krishna, Grid connected three-level converters: studies for wave energy conversion, PhD thesis, Uppsala University, 2014.

[73] L. Hai, Modelling wave power by equivalent circuit theory, PhD thesis, Uppsala University, 2016.

[74] E. Lejerskog, Theoretical and experimental analysis of operational wave energy converters, PhD thesis, Uppsala University, 2016.

[75] V. Castellucci, Sea level compensation system for wave energy converters, PhD thesis, Uppsala University, 2016.

[76] M.E. McCormick. Ocean Engineering Mechanics: With Applications. *Cambridge University Press*, 32 Avenue of the Americas, New York, NY 10013-2473, USA, 1st edition, 2010

[77] J. Falnes, A review of wave-energy extraction. *Marine Structures*. 20, 185–201, 2007.

[78] R.G. Dean and R.A. Dalrymple. Water wave mechanics for engineers and scientists, Advanced series on ocean engineering 2:ed. Prentice Hall, Inc. ISBN 981-02-0420-5,1991.

[79] M. Mueller and R. Wallace. Enabling science and technology for marine renewable energy. *Energy Policy*. 36(12), 4376-4382, 2008.

[80] C.L. Bretschneider. On wind generated waves, topics in ocean engineering. *Gulf Publishing*, Houston, 37-41, 2006

[81] M.A. Mueller and N.J. Baker. A low speed reciprocating permanent magnet generator for direct drive wave energy converters. *International Conference on Power Electronics, Machines and Drives*. 468-473, 2002.

[82] I. Boldea and S.A. Nasar. Linear electric actuators and generators. *Cambridge University Press*, Cambridge, United Kingdom, 1997.

[83] C. Boström, Electrical systems for wave energy conversion, PhD thesis, Uppsala University, 2011.

[84] B. Ekergård, C. Boström, A. Hagnestål, R. Waters and M. Leijon. Experimental results from a linear wave power generator connected to a resonance circuit. *Wiley Interdisciplinary Reviews: Energy and Environment*, 2012

[85] C. Boström, B. Ekergård, M. Leijon, Electric resonance-rectifier circuit for renewable energy conversion. *Applied Physics Letters*. 100, 43511, 2012.

[86] Barstow, S.F.; Mørk, G.; Lønseth, L.; Mathisen, J.P.; Schjølberg, P. The role of satellite wave data in the WORLDWAVES project. In *Proceedings of the 5th International Symposium on Ocean Wave Measurement and Analysis*. Madrid, Spain, 2005.

[87] R. Waters, J. Engström, J. Isberg, M. Leijon. Wave climate off the Swedish west coast. *Renewable Energy*. 34, 1600–1606, 2009.

Acta Universitatis Upsaliensis

Digital Comprehensive Summaries of Uppsala Dissertations from the Faculty of Science and Technology 1443

Editor: The Dean of the Faculty of Science and Technology

A doctoral dissertation from the Faculty of Science and Technology, Uppsala University, is usually a summary of a number of papers. A few copies of the complete dissertation are kept at major Swedish research libraries, while the summary alone is distributed internationally through the series Digital Comprehensive Summaries of Uppsala Dissertations from the Faculty of Science and Technology. (Prior to January, 2005, the series was published under the title "Comprehensive Summaries of Uppsala Dissertations from the Faculty of Science and Technology".)

Distribution: publications.uu.se
urn:nbn:se:uu:diva-305650

ACTA
UNIVERSITATIS
UPSALIENSIS
UPPSALA
2016